Two-stage Robust Wireless Body Area Network Design

Mohammad Ali Raayatpanah[a], Atefeh Abdolah Abyaneh[a], Jocelyne Elias[b] and Fabio Martignon[c,*]

[a]Mathematical Sciences and Computer, Kharazmi University; Tehran, Iran.
[b]Department of Computer Science and Engineering, University of Bologna, Bologna, Italy
[c]Department of Management, Information and Production Engineering, University of Bergamo, Bergamo, Italy

ARTICLE INFO

Keywords:
Wireless Body Area Networks (WBANs)
Robust optimization
Data rate uncertainty
Energy-efficient routing

ABSTRACT

The Internet of Things (IoT) has reshaped technology paradigms through the integration of intelligent components like sensors, paving the way to the development of Wireless Body Area Networks (WBANs) specifically tailored for healthcare applications. However, designing an efficient WBAN requires addressing several challenges, including energy-efficient routing and data rate uncertainty. In response to these challenges, this paper proposes a novel approach — a two-stage robust programming formulation — for WBAN design. The primary aim is to minimize both energy consumption and relay placement costs, all while accounting for the inherent uncertainty in data rates. The proposed formulation explicitly addresses data rate uncertainties, leveraging robust optimization techniques to handle this uncertainty. We prove that efficiently solving an approximation of this robust formulation is achievable. Numerical results, measured in a set of realistic WBAN scenarios, demonstrate the effectiveness of the introduced two-stage robust programming formulation in achieving notable reductions in energy consumption and relay placement costs within the context of WBANs.

1. Introduction

The Internet of Things (IoT) has radically transformed technology, particularly in the healthcare domain, by enabling the integration of intelligent sensors. This has paved the way for the *Internet of Medical Things (IoMT)*, a technological advancement that significantly enhances healthcare services and reduces operational costs through wireless medical devices [Kumar et al., 2021, Razdan and Sharma, 2022]. A critical component of IoMT is *Wireless Body Area Networks (WBANs)*, which rely on wearable body sensors for real-time patient monitoring, collection of physiological data, and the facilitation of remote healthcare services. WBANs enable continuous surveillance of patients' health signals, facilitating early identification of medical emergencies and enabling prompt intervention [Lata et al., 2021, Elhayatmy et al., 2018, Sharma and Kang, 2020].

These networks are built around sensors placed on or within the human body, which wirelessly transmit medical data to a remote server or a personal device, such as a smartphone or smartwatch. The devices can then classify physiological signals as normal or abnormal and take appropriate actions, such as issuing warnings or notifying healthcare providers or family members. Figure 1 illustrates a typical WBAN, with multiple biosensors deployed on the human body. The integration of WBANs into daily life has revolutionized patient monitoring, ensuring seamless, real-time health tracking and early detection of abnormalities during normal activities [Akkaş et al., 2020, Zhang and Dong, 2023]. This approach has enabled healthcare professionals to adopt more proactive treatment strategies based on continuous data analysis, leading to early diagnoses and targeted interventions [d'Angelis et al., 2022].

Despite these advantages, the deployment of WBANs faces several critical challenges. Notably, ensuring the continuous operation of all sensors is crucial for effective health monitoring. Sensor malfunctions due to energy depletion or hardware failures can result in missed data, jeopardizing the patient's health, particularly when treatment decisions rely on real-time sensor data. As such, maintaining the longevity and reliability of WBANs is vital [Paganelli et al., 2022]. The performance of WBANs is directly influenced by the energy consumption of sensors and the quality of their data transmission capabilities, which are impacted by the wireless technology in use (e.g., Bluetooth Low Energy (BLE) or Wi-Fi) [Swaroop et al., 2019].

*Corresponding author
raayatpanah@khu.ac.ir (M.A. Raayatpanah); Std_Abyaneh@khu.ac.ir (A.A. Abyaneh); jocelyne.elias@unibo.it (J. Elias); fabio.martignon@unibg.it (F. Martignon)
ORCID(s): 0000-0002-3303-0981 (M.A. Raayatpanah); 0000-0003-2691-9827 (F. Martignon)

In this context, there is an urgent need to design energy-efficient network topologies and routing protocols that ensure continuous, reliable operation of WBANs over extended periods. Researchers have proposed various solutions, including energy-aware topology design, Quality-of-Service (QoS)-aware performance improvements, reliable routing protocols, and cross-layer media access control mechanisms [Ullah et al., 2022, 2019, Zhou et al., 2017, Kaur and Singh, 2017]. These studies emphasize the importance of energy-efficient routing to mitigate issues related to energy consumption and ensure optimal sensor performance in WBANs.

1.1. Motivation

Wireless Body Area Networks have become essential for healthcare applications, enabling remote and real-time monitoring of patients' health conditions. However, their adoption faces significant challenges, particularly due to energy consumption, traffic demand uncertainty, and dynamic patient conditions. Neglecting such uncertainties may result in infeasible or inefficient solutions, compromising the reliability of the network and, consequently, patient health. Addressing these issues is crucial for ensuring the reliability, efficiency, and practicality of WBAN deployment in healthcare scenarios.

A primary issue is traffic/demand uncertainty, where body sensors produce data at variable rates influenced by event-driven operations or dynamic patient conditions [Keoh et al., 2007, Mitra et al., 2012, Chen et al., 2010, D'Andreagiovanni and Nardin, 2015]. For example, cardiac sensors may generate bursts of data during critical events, such as arrhythmias, while remaining dormant otherwise [D'Andreagiovanni and Nardin, 2015]. Ignoring this variability risks network designs that fail under real-world conditions, leading to data loss, delays, and compromised patient outcomes. Overestimating data rates may result in inefficient resource utilization, while underestimating them risks overloading relays or network bottlenecks, causing packet drops [Flushing and Di Caro, 2013]. The repercussions of such failures are particularly severe when vital data, such as ischemia detection, is involved. These issues highlight the necessity of robust optimization models that proactively account for traffic uncertainties and ensure feasible, resilient, and efficient WBAN designs [Khan et al., 2020].

Energy efficiency is another critical concern for WBANs, particularly due to the limited capacity and non-replaceable nature of many sensor batteries [Chen et al., 2010, Khan et al., 2020]. This challenge is even more pronounced for implanted sensors, where replacing batteries may require invasive procedures. Multi-hop communication has been proposed as an energy-efficient strategy to mitigate this issue by reducing transmission distances [Jawad and Khurshid, 2022]. Intermediate relay nodes can extend the network's lifetime and reduce energy consumption. However, this approach introduces additional complexities, such as optimal relay placement and routing, which must balance energy usage, traffic load, and network lifetime [Vyas et al., 2021, Raayatpanah et al., 2023]. Without careful optimization, relays may experience traffic congestion, leading to higher energy depletion and reduced network reliability [Chen et al., 2010].

Patient mobility further complicates WBAN deployment. Movements such as walking, running, or sitting alter the network's topology and degrade communication reliability [Samanta and Misra, 2018]. Topological changes may cause frequent disconnections or increased packet delays, threatening the quality of real-time health monitoring. Ensuring continuous connectivity and stable performance during patient mobility is vital for applications like post-operative care or monitoring chronic illnesses [Raayatpanah et al., 2023].

Finally, existing WBAN design approaches often rely on deterministic assumptions about network conditions [Keoh et al., 2007], failing to account for the inherently unpredictable nature of real-world scenarios. Biosensors configured in event-driven modes [Chen et al., 2010] generate highly variable data rates, creating uncertainty that complicates effective planning [Flushing and Di Caro, 2013]. We will show that addressing such uncertainty through robust optimization frameworks enables WBANs to maintain energy efficiency and reliable data transfer despite fluctuating network conditions.

This study builds on prior work by developing a novel two-stage robust optimization framework for WBANs. This framework simultaneously addresses traffic/demand uncertainty, energy consumption, and relay placement. By modeling traffic variability explicitly, the proposed method ensures reliable network performance under worst-case conditions while minimizing energy consumption and placement costs [D'Andreagiovanni and Nardin, 2015, Khan et al., 2020]. Furthermore, compared to existing single-stage approaches, our two-stage optimization strategy dynamically adjusts routing and relay placements, enhancing adaptability to real-time changes in network conditions [Raayatpanah et al., 2023].

In summary, the motivation for this work lies in addressing these interconnected challenges—traffic/demand uncertainty, energy efficiency, patient mobility, and adaptability—to provide a practical, reliable, and resilient WBAN

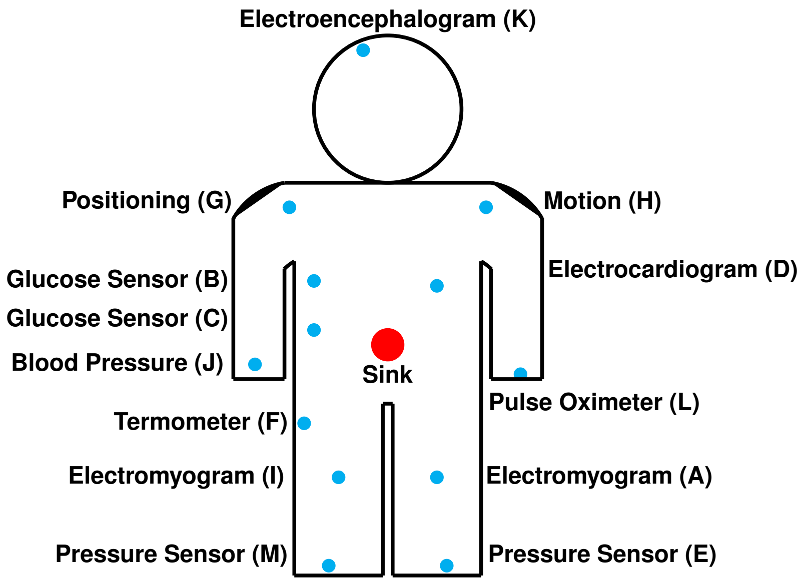

Figure 1: Schematic example of a WBAN with different types of biosensors deployed on the human body.

solution. By leveraging robust optimization techniques, we offer significant advancements that ensure the feasibility and robustness of WBANs in realistic and dynamic healthcare scenarios.

1.2. Contributions

In this paper, we focus on *robust optimization* to address demand uncertainty, striving for solutions that remain feasible for all demand vectors within estimated uncertainty sets. Our focus is on capacity planning for WBANs, jointly optimizing topology and routing under traffic uncertainty. The problem is naturally expressed as a two-stage stochastic programming problem with recourse [Sen et al., 1994, Lisser et al., 1999, Riis and Andersen, 2002]. The first stage involves determining relay nodes capacities, while decisions related to relay placement and traffic routing are made in the second stage to satisfy the observed demands. As a result, routing inherently incorporates stochastic elements due to uncertainty in data rates. This problem represents a specific instance of broader network design formulations where demands and, potentially, travel times are uncertain parameters. With the transmission of critical data in WBANs, a two-stage robust programming formulation emerges as a more suitable framework for adapting to uncertain data transmission rates via relays.

Our main contributions revolve around the proposed model and methodology, and can be summarized as follows:

- **Uncertainty Modeling for WBANs**: We propose a novel uncertainty-modeling framework tailored specifically for WBANs. Unlike previous studies that often overlook the dynamic nature of biosensor data and traffic fluctuations, our framework effectively captures and represents uncertainty associated with various biosensor data types in diverse scenarios.

- **Robust Optimization Approach**: Leveraging robust optimization techniques, we address the challenge of demand uncertainty in WBAN design. By formulating a two-stage robust programming framework, we ensure that solutions remain feasible for all possible demand vectors within estimated uncertainty sets, enhancing the reliability and resilience of WBANs for continuous and dependable communication between biosensors and sinks. We further demonstrate that efficiently solving an approximation of this robust formulation is achievable.

- **Energy-Aware WBAN Design**: Additionally, our work focuses on optimizing the design of Energy-Aware WBANs, aiming to minimize network energy consumption while making optimal routing decisions among an optimal number of installed relays. By integrating uncertainty modeling and robust optimization, we provide a comprehensive solution that balances energy efficiency with practical considerations.
- **Computational Experiments**: To validate the effectiveness of the proposed models and algorithms, we conduct computational experiments using realistic WBAN instances. To assess our approach, we compare it with two baseline models: a Deterministic Model and a Worst Case Scenario approach, highlighting the flexibility and robustness of our method in comparison. The evaluation measures the network's performance under varying data rates and traffic conditions.

1.3. Paper Organization

The remainder of this paper is organized as follows: Section 2 provides an overview of related works. Section 3 introduces the network model and discusses the energy model considered in our study. Following this, Section 4 presents the Mixed-Integer Linear Programming (MILP) framework developed to optimize relay node placement and determine efficient routing strategies amidst uncertain biosensor data generation. Section 5 details the formulation of a two-stage robust optimization approach, and illustrates an example scenario that shows the effectiveness of such approach. Section 6 presents the WBAN scenario, providing insight into the network's topology and the specific scenario considered for our numerical evaluation. Subsequently, Section 7 illustrates and discusses computational experiments comparing Robust solutions with Deterministic ones. Finally, in Section 8, we summarize the key findings and implications of our research, identifying promising research directions.

2. Related work

To address the challenges of wireless sensor networks for healthcare applications, extensive research has focused on optimizing various aspects of network performance. Prior works have investigated strategies to improve energy efficiency for biosensor nodes, establish secure and energy-efficient frameworks for e-healthcare, optimize energy consumption in wireless body area networks (WBANs), and develop mathematical models for body area network topology design [Cao et al., 2009, Chen et al., 2010, Liu et al., 2013, Peter et al., 2016, Khan and Pathan, 2018, Alshaheen and Takruri-Rizk, 2017, Kanthi and Dilli, 2023, Hu et al., 2016]

More recent studies have expanded these efforts. For instance, the work in [Ghosh, 2023] explores optimal relay node deployment in WBANs to enhance energy efficiency and network lifetime, demonstrating that linear midpoint placement may not always yield optimal results. Similarly, [Panhwar, 2021] employs a Genetic Algorithm to optimize routing paths for continuous health monitoring, minimizing energy consumption while ensuring reliable data transmission. Moreover, [Patra, 2024] introduces a mathematical model utilizing the Free Search Krill Herd algorithm for relay node placement, complemented by a Harmony Search algorithm for routing, targeting improved energy efficiency and reliability.

Dynamic scheduling and resilience principles from related fields also offer valuable insights. Han et al. [Han et al., 2015] investigate on-line supply chain scheduling in dynamic environments, focusing on minimizing makespan and delivery costs. Their exploration of scheduling decisions under incomplete information aligns with the challenges of data transmission scheduling in WSNs. Similarly, Zhang et al. [Zhang and van Luttervelt, 2011] propose principles for resilient manufacturing systems, emphasizing adaptability and recovery from failures. These insights parallel the need for robust and adaptable network design in healthcare applications. Furthermore, Wang et al. [Wang et al., 2019] present an integrated approach to resilience in transportation systems, combining infrastructure recovery with flow planning, which informs the development of robust strategies for WSN routing and relay placement.

Adaptability in resource-constrained systems is further highlighted by Zhang et al. [Zhang et al., 2018], who propose an underactuated self-reconfigurable robot architecture featuring passive joints to enhance resource efficiency and resilience. Their two-phase reconfiguration planning and scheduling model demonstrates how adaptability can be achieved under resource constraints, providing useful analogies for WSN optimization.

In the context of mobile WBANs, where dynamic body movements degrade link quality and network performance, several innovative frameworks have emerged. The authors in [Samanta and Misra, 2018] proposed an energy-efficient distributed framework for managing network connectivity and minimizing data dissemination delays in opportunistic WBANs. Their approach accounted for irregular body movements, such as walking and running, significantly improving throughput and reducing energy consumption compared to existing solutions. Similarly, [Samanta et al., 2024] presented LALB, a packet loss detection algorithm, alongside a joint optimization framework to mitigate mobility's adverse effects on network performance, demonstrating significant improvements in power consumption and throughput through simulations.

Despite these advancements, existing works often fail to address data rate uncertainties between biosensor-sink pairs comprehensively. Neglecting such uncertainties can lead to impractical solutions, particularly in healthcare applications where reliability is paramount [D'Andreagiovanni and Nardin, 2015, Ben-Tal et al., 2009a]. This gap underscores the necessity of robust optimization methodologies to accommodate uncertainty while ensuring network reliability and efficiency.

The operations research community has extensively explored uncertainty in mathematical programming. Probabilistic approaches, such as scenario-based stochastic optimization [Birge and Louveaux, 2011], optimize the expected value of objective functions under the assumption of known probability distributions. However, these methods face limitations, including high computational complexity, sensitivity to uncertainty outcomes, and reliance on potentially inaccurate probabilistic models [Bertsimas and Sim, 2003, Ben-Tal et al., 2009b]. Robust optimization offers a compelling alternative by focusing on worst-case scenarios within predetermined uncertainty sets [Ben-Tal and Nemirovski, 1998, El Ghaoui et al., 1998, Bertsimas and Sim, 2004]. This methodology ensures feasible and efficient solutions even under severe uncertainty.

A notable contribution in this domain is [D'Andreagiovanni and Nardin, 2015], which proposed a single-stage robust optimization model for WBAN topology and routing under traffic uncertainty. Employing a scenario-based min-max approach, the model minimizes the maximum deviation between proposed and optimal solutions across all scenarios. However, the reliance on scenario-based uncertainty sets may not encompass all potential demand realizations, limiting its applicability.

Several methodologies addressing uncertainty in IoT networks have been highlighted, including fault-tolerance mechanisms [Samanta et al., 2021]. In IoT systems, [Hussain et al., 2019] evaluated classifiers like Decision Tree and Random Forest for robustness against data quality issues, while [Alwhishi et al., 2022] proposed multi-valued model checking for verifying IoT services under uncertainty. Additionally, [Xu et al., 2022] developed Evidential Multiview Deep Learning (EMDL), a method synthesizing multiple features for reliable decision-making, demonstrating superior performance in synthetic and real-world datasets.

Building on this foundation, our work introduces a two-stage robust optimization model tailored for WBANs. This approach surpasses single-stage methods by accommodating real-time adjustments to uncertain parameters, providing flexibility and adaptability to varying network conditions. Two-stage optimization enables the formulation of a robust counterpart to the original problem in the first stage, addressing wide-ranging uncertainties, and the fine-tuning of solutions in the second stage to optimize performance under specific realizations [Ben-Tal et al., 2004, Atamtürk and Zhang, 2007].

Our methodology diverges significantly from [Amjad et al., 2020], which employed stochastic programming to optimize energy efficiency in WBANs without requiring channel state information. While their work addressed single-hop routing and utilized generalized gamma distributions to model uncertainties, our approach emphasizes multi-hop routing. This strategy integrates intermediary biosensors to create shorter connections, reduce energy consumption, and extend network lifespans. Moreover, our robust optimization framework eliminates the need for known probability distributions, enhancing solution reliability and adaptability.

Finally, our prior work [Raayatpanah et al., 2023] explored relay-based multi-hop communication to optimize device positioning and routing in WBANs, demonstrating improved energy efficiency and data transfer reliability. Expanding on this, the current study incorporates a novel two-stage robust programming framework that simultaneously addresses energy consumption, relay placement costs, and data rate uncertainties. By leveraging robust optimization techniques, we achieve substantial reductions in energy consumption and relay placement costs, offering a practical and resilient solution for WBANs in realistic healthcare scenarios.

3. System Model

In this section we first introduce the network model (section 3.1) and then the energy model (section 3.2) considered in our work.

Notation	Meaning
B	Biosensor node set
R	Relay node set
K	Set of capacity choices available for relays
s	Sink node
$\hat{A}$	Set of links between relay nodes
$\tilde{A}$	Set of links between relay nodes, biosensor nodes and sink
$FS(i)$	Forward star of node i
$\widetilde{FS}(b)$	Set of relays that can be assigned to biosensor b
$RS(i)$	Reverse star of node i
$\widetilde{RS}(s)$	Set of relays that can be assigned to the sink s
E_{RXelec}	Received energy
E_{TXelec}	Transmission energy
E_{amp}	Energy for the transmission amplifier
α	Objective function coefficient
v_i^k	Capacity of relay i of type k
c_i^k	Cost for installing relay i with capacity v_i^k
U	Maximum number of relays that can be installed (*candidate sites*)
g	Maximum number of relays that can establish a link with sink s
p	Total number of transmitted/received bits
d^b	Uncertain traffic generated by biosensor b [bits/s]
$\mathcal{U}_d$	Uncertain set of traffic generated by all biosensors
n_{ij}	Path loss coefficient for link (i,j)
D_{ij}	Distance between two nodes i, j
a_{bi}	0-1 connectivity parameter between biosensor b and relay i
e_{is}	0-1 connectivity parameter between relay i and sink s

Variable	Description
$x_{bi}(d^b)$	0-1 variable indicating if biosensor $b \in B$ is assigned to relay $i \in R$
$z_{ij}^b(d^b)$	0-1 variable indicating if link $(i,j) \in \hat{A}$ is used by biosensor $b \in B$
$f_{is}^b(d^b)$	0-1 variable indicating if link $(i,s) \in \tilde{A}$ is used by biosensor $b \in B$
x_{is}	0-1 variable indicating if relay $i \in R$ is assigned to sink s
y_i^k	0-1 variable indicating if relay i of type $k \in K$ is installed in candidate site $i \in R$

Table 1
Notations, parameters and variables definition

3.1. Network Model

The wireless body area network considered in this study models a typical *standing* scenario where arms hang along each side of the body. This scenario's topology includes various biosensors positioned strategically for different detection purposes, along with relay nodes that assist biosensors by acting as data transmitters towards the sink. Consequently, a multi-hop routing strategy is employed to transfer data from biosensors to the sink, with each biosensor-sink path containing at least one relay node.

Biosensors, denoted as B, are deployed at predefined locations based on their specific applications, as illustrated in Figure 1. The sink node (terminal) is situated at the origin of the coordinate system [Raayatpanah et al., 2023]. In fact, the locations of biosensors and the sink node are predetermined. A summary of the notations for all the parameters and variables utilized in this paper is provided in Table 1.

The topology configuration for the WBAN under consideration can be represented by a directed graph $G = (V, A)$. The node set V encompasses a collection of biosensors B that generate biomedical data and transmit it to the sink node s using a set of intermediate relay nodes R. Each biosensor $b \in B$ generates d^b units of data. The actual data value is assumed to be uncertain, with $d \in R_+^{|B|}$ lying within a given polytope.

The multi-hop routing approach implemented in this model necessitates the placement of at least one relay $i \in R$ along the path from biosensor $b \in B$ to the sink s. Therefore, relays play a crucial role in the WBAN design. As a consequence, the first set of decisions in our model focuses on the selection of relay nodes. We assume that relay nodes may exhibit non-uniform characteristics: they could vary in type, implying different capacities and costs. For instance, if relay $i \in R$ of type $k \in K$ is installed, it will have a corresponding capacity denoted as v_i^k and a cost indicated by c_i^k. Such cost may represent the purchasing or monetary cost, as well as the maintenance cost (when relay i is not a one-time device) of the relay node with capacity v_i^k. This decision-making process aims to optimize the network's performance by selecting the most suitable relay nodes based on their capacities and costs.

While using a significant number of relays can significantly reduce network energy consumption and enhance the network's quality of service, it can also increase radiation absorption in body tissues, potentially causing harm to sensitive organs due to reduced blood flow and the growth of certain bacteria [Ahmed et al., 2020, Zhou et al., 2017]. Therefore, a constraint is imposed on the maximum number of relays that can be installed. In our model, there is a maximum of U available candidate sites for relay installation. Another constraint limits the number of relays that can establish connections with the sink to $g \geq 0$. Thus, g relays are allowed to establish links with the sink s.

We assume that all biosensors transmit data through at least one relay. However, our formulation can be easily modified as we specify below to enable direct communication between nearby biosensors and the sink, if that is the optimal solution.

In our scenario, the Communication Range (CR) is defined for each biosensor b and the sink s, along with binary coverage parameters a_{bi} and e_{is}, respectively. This means that biosensors and the sink can only communicate with relays installed within their communication range. Consequently, $a_{bi} = 1$ if biosensor b can establish a link with relay i; otherwise, $a_{bi} = 0$. Similarly, $e_{is} = 1$ when relay i can establish a connection with the sink s; otherwise, $e_{is} = 0$.

The enforcement of the communication range in establishing wireless links between devices yields two sets of eligible links, denoted as $\hat{A}$ and $\tilde{A}$, where $A = \hat{A} \cup \tilde{A}$. We define $\hat{A} \subseteq \{(i,j)|i,j \in R\}$ as the set of wireless links with both incident nodes in R, and $\tilde{A} \subseteq \{(b,j) \cup (j,s)|b \in B, j \in R\}$ as the set that includes all eligible biosensor-relay and relay-sink assignments.

For each relay $i \in R$, we define the forward star as $FS(i) = \{j|(i,j) \in A\}$ and the reverse star as $RS(i) = \{h|(h,i) \in A\}$. Similarly, we define $\widetilde{FS}(b) = \left\{i|(b,i) \in \tilde{A}\right\}$ to represent the set of relays that can be assigned to biosensor $b \in B$. It is important to note that in order to enable a direct communication between biosensors and the sink, we just need to modify $\widetilde{FS}(b)$ as $\widetilde{FS}(b) = \left\{i|(b,i) \in \tilde{A} \cup (b,s)\right\}$. We also define $\widetilde{RS}(s) = \left\{i|(i,s) \in \tilde{A}\right\}$ as the set of relays that can be assigned to the sink s.

3.2. Energy Model

To extend the battery life of nodes within WBANs, it is imperative to reduce energy consumption. The primary contributors to energy utilization in WBANs include data transmission, reception, sensing, and processing. Therefore, in line with the approach outlined in [Elias, 2014, Reusens et al., 2009, Elias et al., 2013], our primary focus is on diminishing the energy expenditure of wireless nodes, particularly by targeting the communication-related energy incurred during data transmission and reception.

To quantify the energy utilization of individual devices, we use E_{TXelec} and E_{RXelec} to denote the energy consumption associated with transmitting and receiving a single bit of data. Employing this methodology, we can calculate the energy required by wireless device i to transmit p bits to device j over the link (i,j) as follows:

$$E_{trans}(i,j) = p\left[E_{TXelec} + E_{amp}(n_{ij})D_{ij}^{n_{ij}}\right].$$

Similarly, the energy consumed by a relay or the sink for receiving p bits can be computed as:

$$E_{rec} = pE_{RXelec}.$$

Here, $E_{amp}(n_{ij})$, D_{ij}, and p represent the energy for the transmission amplifier, which depends on the path loss coefficient n_{ij}, the distance between nodes i and j, and the total number of transmitted/received bits, respectively.

4. Mixed-Integer Linear Programming formulation

This section presents the Mixed-Integer Linear Programming (MILP) framework designed to optimize the placement of relay nodes and identify the most efficient routing strategies in the presence of uncertain biosensor data generation. The decision variables are defined below.

We first introduce an integer decision variable, x_{bi}, acting as an assignment variable for biosensor b. This sensor produces uncertain traffic denoted by d^b. We express this variable as follows:

$$x_{bi}(d^b) = \begin{cases} d^b, & \text{if biosensor } b \in B \text{ is assigned to relay } i \in R, \\ 0, & \text{otherwise.} \end{cases} \tag{1}$$

Since routing is unsplittable, $x_{bi} = d^b$ means that biosensor $b \in B$ is assigned to only one relay $i \in R$, hence all (uncertain) data generated by b is routed/transmitted to relay i. Note that d^b takes integer values, which is not a limiting assumption since it is expressed in bits/s.

We also define two additional unsplittable flow variables, z^b_{ij} and f^b_{is}, which are associated with links and indicate whether all uncertain data generated by biosensor b is routed through the given link:

$$z^b_{ij}(d^b) = \begin{cases} d^b, & \text{if link } (i,j) \in \hat{A} \text{ is used by biosensor } b \in B, \\ 0, & \text{otherwise,} \end{cases} \tag{2}$$

$$f^b_{is}(d^b) = \begin{cases} d^b, & \text{if link } (i,s) \in \tilde{A} \text{ is used by biosensor } b \in B, \\ 0, & \text{otherwise.} \end{cases} \tag{3}$$

We also define the binary variable x_{is} to indicate the assignment of relay i to sink s:

$$x_{is} = \begin{cases} 1, & \text{if relay } i \in R \text{ is assigned to sink } s, \\ 0, & \text{otherwise.} \end{cases} \tag{4}$$

Moreover, we introduce the binary variable y^k_i, which determines the installation of relay i of type k:

$$y^k_i = \begin{cases} 1, & \text{if relay } i \text{ of type } k \in K \text{ is installed in candidate site } i \in R, \\ 0, & \text{otherwise.} \end{cases} \tag{5}$$

Once the decision variables have been defined, we can now proceed to establish the constraints representing feasible solutions for our problem.

To ensure that each biosensor b transmits data via a single path, we enforce that it connects to exactly one relay, in accordance with the definition of the integer variable x_{bi}:

$$\sum_{i \in \widetilde{FS}(b)} x_{bi} = d^b, \quad \forall b \in B. \tag{6}$$

We need to ensure that the uncertain generated data transmitted by biosensors to the sink at each relay is balanced by the data received from biosensors and forwarded to other relays. This is achieved by applying the following flow balance constraint:

$$\sum_{j \in FS(i)} z^b_{ij} - \sum_{h \in RS(i)} z^b_{hi} = x_{bi} - f^b_{is}, \quad \forall b \in B, i \in R. \tag{7}$$

Additionally, constraints are imposed to ensure that biosensors can only establish connections with relays that are both installed and eligible based on their capacity:

$$x_{bi} \leq d^b \sum_{k \in K} y^k_i a_{bi}, \quad \forall b \in B, i \in R. \tag{8}$$

The following constraints are applied to the sink assignment variables, restricting the sink coverage by relay type and setting an upper limit on the number of relays assigned to the sink:

$$x_{is} \leq \sum_{k \in K} y^k_i e_{is}, \quad \forall i \in R, \tag{9}$$

$$\sum_{i \in \widetilde{RS}(s)} x_{is} \leq g. \tag{10}$$

Relays facilitate data transmission from biosensors to the sink, subject to link availability, as per the following constraint:

$$f_{is}^b \leq d^b x_{is} e_{is}, \quad \forall b \in B, i \in R. \tag{11}$$

Constraint (12) ensures that at most one relay of capacity type k can be installed at each candidate site i:

$$\sum_{k \in K} y_i^k \leq 1, \quad \forall i \in R. \tag{12}$$

Additionally, constraints (13) and (14) limit the total number of relay nodes in the network and ensure that incoming traffic to relay nodes does not exceed their capacity.

$$\sum_{i \in R} \sum_{k \in K} y_i^k \leq U, \tag{13}$$

$$\sum_{b \in B} \sum_{h \in RS(i)} z_{hi}^b + \sum_{b \in B} x_{bi} \leq \sum_{k \in K} v_i^k y_i^k, \quad \forall i \in R. \tag{14}$$

In the domain of WBANs, effectively managing data traffic demands is crucial, mirroring the complex challenges posed by demand uncertainty. This uncertainty in WBANs arises from various factors, primarily due to their prominent application in healthcare. Here, data transmission requirements exhibit substantial variability, contingent on the physiological state, activity levels, and health conditions of the monitored individuals, creating uncertain data loads akin to those observed in traditional telecommunications networks. Furthermore, inherent resource constraints within WBAN devices necessitate the deployment of adaptive communication protocols designed to optimize energy consumption. This need for adaptability introduces additional layers of variability in data demands as the network continuously adapts to conserve energy, adding a dimension of complexity comparable to demand uncertainties in telecommunications networks.

Addressing demand uncertainty within the WBAN paradigm presents a significant research challenge, akin to the critical issues faced in capacity planning and network design for conventional telecommunications networks. Effectively managing demand variability is not only essential but also crucial for ensuring the efficient and dependable operation of WBANs, especially in life-critical healthcare applications. Even a slight deviation in demand can make routing problems very challenging to solve. Thus, incorporating safety margins into capacity planning becomes imperative, enabling the network to adeptly accommodate fluctuations between planned and actual demand.

Moreover, it is essential to recognize that fluctuations in demand can exert a notable influence on the objective function, potentially resulting in shifts in its value. Our objective is to minimize the expression $C_{Investment} + \alpha C_{Energy}$, where $C_{Investment}$ represents the cost associated with relay capacity investment, computed as $\sum_{j \in R} \sum_{k \in K} c_j^k y_j^k$, and C_{Energy} encompasses three distinct energy consumption components: ET_{trans}^{Bio}, ET_{trans}^{Relay}, and ET_{rec}^{Relay}. These components represent the energy expended during traffic transmission by biosensors, traffic transmission by relays, and traffic reception by relays, respectively. The parameter α plays a pivotal role in our optimization, determining the relative weight attributed to each cost component in the objective function. As a result, variations in demand can significantly influence the overall optimization objective, highlighting the importance of incorporating demand uncertainty comprehensively into our modeling approach.

Therefore, we formulate the Linear Optimization Uncertain (LOU) problem as follows:

$$Z_{LOU} = \min C_{Investment} + \alpha C_{Energy} \qquad (LOU) \tag{15}$$
$$s.t.\ Constraints\ (1) - (14).$$

The robust solution is obtained by solving the following Robust Counterpart problem (RC):

$$
\begin{aligned}
Z_{RC} = \min & \sum_{j\in R}\sum_{k\in K} c_j^k y_j^k + \alpha \max_{d\in\mathcal{U}_d} \Big(\sum_{b\in B}\Big(\sum_{j\in \widetilde{FS}(b)} x_{bj}(ET_{trans}^{Bio}) + \sum_{(i,j)\in R} z_{ij}^b (ET_{trans}^{rel}) + \sum_{j\in\widetilde{RS}(s)} f_{js}^b (ER_{rec}^{sink})\Big)\Big) \\
s.t. & \sum_{i\in \widetilde{FS}(b)} x_{bi} = d^b, && \forall b\in B, \\
& \sum_{j\in FS(i)} z_{ij}^b - \sum_{h\in RS(i)} z_{hi}^b = x_{bi} - f_{is}^b, && \forall b\in B, i\in R, \\
& x_{bi} \le d^b \sum_{k\in K} y_i^k a_{bi}, && \forall b\in B, i\in R,\ d\in\mathcal{U}_d \\
& x_{is} \le \sum_{k\in K} y_i^k e_{is}, && \forall i\in R \\
& \sum_{i\in\widetilde{RS}(s)} x_{is} \le g \\
& f_{is}^b \le d^b x_{is} e_{is}, && \forall b\in B, i\in R, d\in\mathcal{U}_d \\
& \sum_{k\in K} y_i^k \le 1, && \forall i\in R, \\
& \sum_{i\in R}\sum_{k\in K} y_i^k \le U \\
& \sum_{b\in B}\sum_{h\in RS(i)} z_{hi}^b + \sum_{b\in B} x_{bi} \le \sum_{k\in K} v_i^k y_i^k, && \forall\ d\in\mathcal{U}_d, \forall i\in R, \\
& (x,z,f)\in\chi,
\end{aligned}
$$

where χ denotes the set of decision variables x, z, and f as defined by equations (1) through (4).

Hence, in this paper, we adopt the principles of robust optimization to improve the reliability and adaptability of network design and capacity planning in WBANs. Our core premise involves integrating uncertain demand, a key aspect of WBANs, into a predetermined uncertainty set. We establish a robust foundation for our research, exploring optimization strategies that can effectively tackle and mitigate the inherent demand variability in WBANs. This approach takes into account the various sources of demand uncertainty, such as the health conditions and physical states of the monitored individuals. Through our study, we aim to develop both theoretical insights and practical solutions to strengthen WBANs against uncertainties, with a particular focus on enhancing their performance and resilience in healthcare applications and related domains.

5. Two-stage Robust Methodology

As previously discussed (Section 2), in the *single-stage* robust optimization approach, all decision variables must be determined before the uncertain data is realized. However, the network design problem under traffic uncertainty is better suited for expression as a *two-stage* robust optimization approach. This involves formulating a model in which only some of the decision variables are determined as “here and now” decisions, while the remaining variables represent “wait and see” decisions and can adapt to the uncertain outcome.

The *first stage* of the model requires decisions to be made regarding network design and capacity allocation before uncertain demand is realized, while the *second stage* involves making routing decisions after observing the demand [Atamtürk and Zhang, 2007]. This type of problem is commonly referred to as a *two-stage problem with recourse* in stochastic programming literature [Birge and Louveaux, 2011]. On the other hand, in single-stage robust optimization, all decisions are made at the beginning, considering the worst-case scenario for the uncertain parameters. Two-stage robust optimization offers several advantages over single-stage robust optimization under demand uncertainty. Firstly, it allows for less conservative solutions by deferring a subset of decisions, thus reducing the probability of infeasibility for a robust solution under random demand vectors. Secondly, the two-stage approach can handle uncertainties in various parameters. Finally, despite the increased computational complexity, the two-stage approach can provide upper bounds on the probability of infeasibility, allowing for quicker solution times and slightly more conservative solutions [Ben-Tal and Nemirovski, 1999, Ben-Tal et al., 2004, Atamtürk and Zhang, 2007]. It typically involves the use of uncertainty sets, such as Gaussian processes, to represent the uncertainty of demand. The approach has been applied to various domains, including energy management, relief network design, water treatment, and supply chain management [Atamtürk and Zhang, 2007, Kammammettu and Li, 2020, Jabbarzadeh et al., 2019, Huang et al., 2021].

We develop the robust formulation for the problem under the assumption that the demand d belongs to a given uncertainty set, $\mathcal{U}_d$, where $\mathcal{U}_d$ is closed, convex, and bounded. Given this uncertainty, we naturally separate decision variables y prior to variables x, f, and z. Since the coefficient matrix of variables x, f, and z is not uncertain, our problem becomes a stochastic problem with fixed recourse [Ben-Tal et al., 2004]. The Adjusted Robust Counterpart problem (ARC) is introduced as the robust counterpart for a stochastic problem with recourse [Ben-Tal et al., 2004]. Hence, if we let $\gamma = \max_{d\in\mathcal{U}_d}(\sum_{b\in B}\big(\sum_{j\in\widetilde{FS}(b)} x_{bj}(ET^{Bio}_{trans}) + \sum_{(i,j)\in R} z^b_{ij}(ET^{rel}_{trans}) + \sum_{j\in\widetilde{RS}(s)} f^b_{js}(ER^{sink}_{rec})\big))$, we can obtain the following (ARC) of the LOU problem:

$$
\begin{aligned}
& Z_{ARC} = \min \sum_{j\in R}\sum_{k\in K} c^k_j y^k_j + \alpha\gamma \\
& s.t. \sum_{k\in K} y^k_i \le 1, \quad \forall i \in R, \\
& \sum_{i\in R}\sum_{k\in K} y^k_i \le U, \\
& y^k_i \in \{0,1\}, \qquad \forall k \in K, i \in R
\end{aligned}
$$

$$
\forall\ d \in \mathcal{U}_d,\ \text{there exists } (x,z,f) \text{ s.t. }
\begin{cases}
\sum_{b\in B}\big(\sum_{j\in\widetilde{FS}(b)} x_{bj}(ET^{Bio}_{trans}) + \sum_{(i,j)\in R} z^b_{ij}(ET^{rel}_{trans}) + \\
\sum_{j\in\widetilde{RS}(s)} f^b_{js}(ER^{sink}_{rec})\big) \le \gamma, \\
\sum_{i\in\widetilde{FS}(b)} x_{bi} = d^b, \qquad \forall b \in B, \\
\sum_{j\in FS(i)} z^b_{ij} - \sum_{h\in RS(i)} z^b_{hi} = x_{bi} - f^b_{is}, \qquad \forall b \in B, i \in R, \\
x_{bi} \le d^b \sum_{k\in K} y^k_i a_{bi}, \qquad \forall b \in B, i \in R, \\
x_{is} \le \sum_{k\in K} y^k_i e_{is}, \qquad \forall i \in R \\
\sum_{i\in\widetilde{RS}(s)} x_{is} \le g, \\
f^b_{is} \le d^b x_{is} e_{is}, \quad \forall b \in B, i \in R, \\
\sum_{b\in B}\sum_{h\in RS(i)} z^b_{hi} + \sum_{b\in B} x_{bi} \le \sum_{k\in K} v^k_i y^k_i, \qquad \forall i \in R, \\
(x,z,f) \in \chi.
\end{cases}
$$

The ARC offers greater flexibility than the RC, with a larger feasible set that allows for better optimal value while still meeting all constraints ($z_{ARC} \le z_{RC}$). However, this increased flexibility comes at the cost of losing the favorable complexity results demonstrated in [Ben-Tal et al., 2004], which proves that the ARC problem for an LP with polyhedral uncertainty is NP-hard. Our research concentrates on determining the conditions within the uncertainty set that result in a manageable ARC for the robust capacity expansion problem. The contrast between the ARC and the RC can indeed be substantial, as illustrated in the following example.

Example 5.1. *Consider Figure 2, which presents a feasible solution for the topology shown in Figure 1. We assume that each relay node is allowed to select a capacity of either 7, 14 or 21. Therefore, the feasibility constraints imply*

the following:
$d^{b_1} \leq 7y^1_{r_1} + 14y^2_{r_1} + 21y^3_{r_1}$
$d^{b_2} \leq 7y^1_{r_2} + 14y^2_{r_2} + 21y^3_{r_2}$
$d^{b_1} + d^{b_2} \leq 7y^1_{r_3} + 14y^2_{r_3} + 21y^3_{r_3}$
Now, let us assume that the demand d is uncertain, but is known to belong to the following polyhedral set [Ben-Tal et al., 2006, Bertsimas and Brown, 2009]:

$$\mathcal{U}_d = \{(d^{b_1}, d^{b_2}) \in R^2 | 0 \leq d^{b_1} \leq 4, 0 \leq d^{b_2} \leq 5, 4d^{b_1} + 3d^{b_2} \leq 19\},$$

as illustrated in Figure 3.

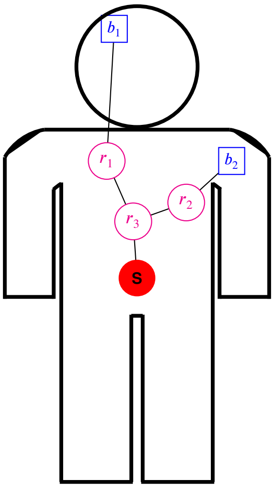

Figure 2: Network planned for example 5.1

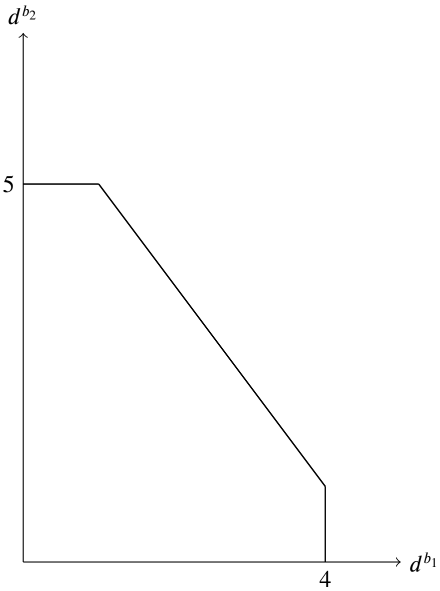

Figure 3: Polyhedral set of uncertainty demand used in example 5.1

A single-stage robust solution for this network is a solution vector y that is feasible for all $\forall\ d \in \mathcal{U}_d$. *Hence, it requires that for relay node* r_1, $4 \le 10y^1_{r_1} + 20y^2_{r_1} + 30y^3_{r_1}$, *for relay node* r_2, $5 \le 10y^1_{r_2} + 20y^2_{r_2} + 30y^3_{r_2}$, *and consequently for relay node* r_3, $9 \le 10y^1_{r_3} + 20y^2_{r_3} + 30y^3_{r_3}$. *These inequalities lead to a minimum capacity of 14 for relay node* r_3.

Let us compare this solution with a two-stage version. In the first stage, we need to determine the capacity variable y that is feasible in the second stage for any $d \in \mathcal{U}_d$. *Then, since* $d^{b_1} + d^{b_2} \le 6$ *for all* $d \in \mathcal{U}_d$, *relay node* r_3 *only needs to satisfy* $6 \le 10y^1_{r_3} + 20y^2_{r_3} + 30y^3_{r_3}$ *to guarantee feasible incoming traffic to relay node* r_3 *in the second stage for any* $d \in \mathcal{U}_d$. *This leads to a minimum capacity of 7 for relay node* r_3.

This simple example illustrates that employing a two-stage robust decision-making approach leads to remarkable 50% reduction in the installed capacity for relay node r_3.

5.1. Uncertainty Sets

The uncertainty model assumes demand, denoted as d, that belongs to a closed, convex, and bounded uncertainty set, $\mathcal{U}_d$. This set does not have any distribution assumptions and models independent uncertainty between demands. For example, this type of uncertainty set can represent the confidence intervals of uncertain quantities.

We assume that, for each $d \in \mathcal{U}_d$, the WBAN design problem is feasible. It should be noted that such assumption regarding the uncertainty sets is equivalent to the relatively complete recourse assumption in the stochastic programming literature [Birge and Louveaux, 2011].

While the RC of an uncertain linear program is usually computationally solvable, the same does not hold true for the ARC [Ben-Tal et al., 2004]. Therefore, in this paper, we consider the following factors to define an uncertainty set that helps in finding a solvable alternative.

It is crucial for the uncertainty set to account for observed data uncertainty. In our case, the set $\mathcal{U}_d$ should accommodate the observed demand fluctuations that frequently occur, while excluding demand realizations that are extremely improbable. The availability of data to formulate and parameterize the uncertainty set is essential. It is desirable to have the ability to adjust the shape of $\mathcal{U}_d$ meaningfully. It is often overlooked but crucial for the resulting formulations or reformulations to be computationally feasible and scalable with the size of instances.

In this study, we define uncertainty sets as deviations from an estimated or nominal value of the uncertain parameter. For instance, when considering the uncertain parameter d we define sets centered around the estimated value $\overline{d}$ and utilize a scalar value ρ_d to manage the confidence in the estimate. Indeed, in the design of wireless body area networks, it is crucial to select an appropriate range of deviation for data parameters according to the specific medical application and biosensors' specifications. Failure to do so can result in the loss of critical biomedical data, potentially endangering patients' lives, as well as the reduction of the network's lifespan [Bertsimas and Sim, 2003, Ben-Tal et al., 2006, Bertsimas and Brown, 2009, Jalilvand-Nejad et al., 2016].

To comprehensively characterize uncertainty while ensuring computational feasibility and scalability, we propose a *polyhedral* uncertain set that can represent a wide range of correlation structures within the uncertain parameter d. This approach enables us to account for correlations between demands of different biosensors in the network, which is a reasonable assumption in wireless networks. By using the polyhedral uncertain set, we can model uncertainty in the demand parameters more accurately, providing a flexible and comprehensive framework for real-world network design scenarios. Since all constraints in the polyhedral set are linear, a solution that proves robust across all scenarios also demonstrates robustness for the convex hull of those scenarios.

$$\text{Polyhedral:} \qquad \mathcal{U}_d = \left\{ d \in \mathscr{R}^{|B|} | d = \overline{d} + \rho_d \hat{d},\ L\hat{d} \le w, \hat{d} \ge 0 \right\} \tag{16}$$

The Polyhedral uncertainty set is a general case of the Budget uncertainty set defined in [Bertsimas and Sim, 2003] as:

$$\mathcal{D} = \{ d \in \mathbb{R}^{\mathcal{H}} : d^h = \overline{d}^h + z^h \hat{d}^h, \sum_{h \in \mathcal{H}} z^h \le \Gamma, 0 \le z^h \le 1, \forall h \in \mathcal{H} \} \tag{17}$$

where $\overline{d}^h$ is the nominal demand for commodity h, $\hat{d}^h$ is the maximum possible deviation from $\overline{d}^h$, and Γ is a parameter that specifies a limit (the budget) on the deviations of all demands at the same time with respect to the nominal values.

It is noteworthy that the *box* uncertain set, which represents the variation of demand around a given nominal demand with a maximal possible deviation, is a special case of the polyhedral uncertain set. As a simple form of uncertain demand, we can consider the following formulation:

$$\text{Box:} \qquad \mathcal{U}_d = \left\{ d \in \mathscr{R}^{|B|} | d = \overline{d} + \rho_d \hat{d}, \|\hat{d}\|_\infty \leq \kappa_\infty \right\} \tag{18}$$

where, in both cases, the parameter $\overline{d}$ represents the nominal or average data rate, while ρ_d denotes the standard deviation or any other measure of dispersion. Additionally, $\hat{d}$ represents a random factor. Typically, the choice of $\hat{d}$ is made based on the level of uncertainty or risk tolerance in the problem and can be derived from historical data, expert judgment, or sensitivity analysis. While the uncertainty set represents an individual demand, it does not consider the low probability of all demands being at their highest value simultaneously. To enhance the precision of the uncertainty set, we can limit the uncertainty by introducing the constraint $\|\hat{d}\|_1 \leq \kappa_1$ into the uncertainty set $\mathcal{U}_d$, resulting in the following *intersection* uncertain set.

$$\text{Intersection:} \qquad \mathcal{U}_d = \left\{ d \in \mathscr{R}^{|B|} | d = \overline{d} + \rho_d \hat{d}, \|\hat{d}\|_\infty \leq \kappa_\infty, \|\hat{d}\|_1 \leq \kappa_1 \right\} \tag{19}$$

The uncertain set represented in (19) provides a close approximation of an uncertain demand set that is spherical in shape, denoted by $\mathcal{U}_d = \left\{ d \in \mathscr{R}^{|B|} | d = \overline{d} + \rho_d \hat{d}, \|\hat{d}\|_2 \leq \kappa_2 \right\}$ in which $\kappa_\infty = \kappa_2$ and $\kappa_1 = \kappa_2 \sqrt{|B|}$. This spherical representation is suitable when all demands are independent normal random variables. For visual reference, when we have two biosensors with uncertain traffic, Figure 4 illustrates an approximation of the unit ball in $\mathscr{R}^2$ with $\kappa_\infty = 1$ and $\kappa_1 = \sqrt{2}$.

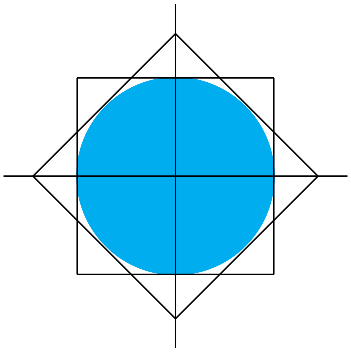

Figure 4: Uncertainty set as the intersection of balls.

Tractable approximate ARC

The adjusted problem, as discussed in [Ben-Tal et al., 2004], presents a significant challenge in terms of finding a solution. To address this, a solution approach was introduced to approximate the problem by constraining the second-stage variable to a specific decision rule of the uncertainty parameter.

The method we propose focuses on the relationship between uncertainty and second-stage variables, providing a more manageable approach to problem-solving. In this context, a decision rule is a function that maps demand realizations to recourse decision variables, capturing the flexibility of these decisions and allowing them to be adjusted to fit the observed demand. Decision rules offer a valuable framework for managing the impact of uncertainty on the decision-making process. They acknowledge that recourse decisions do not need to be fixed before demand is realized and can be adapted to align with actual demand, offering a more dynamic and responsive approach to decision-making under uncertainty. In various works including for example [Wang et al., 2019], the authors pointed out how the dependency between the variables in the two stages can greatly increase the computational overhead. We acknowledge that this dependency increases computational complexity, as second-stage decisions are contingent on both first-stage decisions and uncertainty realizations. To address this, we have implemented a linear approximation for the second-stage variables, as explained in equation (20) hereafter. We define these variables as linear functions of demand realizations, expressed as deviations from nominal values of uncertain parameters, as follows:

$$x_{bi} = d^b \overline{x_{bi}},\ z_{ij}^b = d^b \overline{z_{ij}^b},\ f_{is}^b = d^b \overline{f_{is}^b}, \tag{20}$$

where $\overline{x_{bi}}$, $\overline{z_{ij}^b}$, and $\overline{f_{is}^b}$ represent the new binary decision variables. This linear decision rule approach helps reduce computational overhead by simplifying the dependency structure between stages.

The approach enables a thorough characterization of uncertainty while ensuring computational feasibility and scalability. It is important to note that the decision variables are to be fixed in the first stage, similar to the y variable. By representing the second stage variables of the ARC of the problem with this function, the following problem arises:

$$Z_{ARC} = \min \sum_{j \in R} \sum_{k \in K} c_j^k y_j^k + \alpha\gamma \tag{21}$$

$$s.t. \sum_{k \in K} y_i^k \leq 1, \quad \forall i \in R, \tag{22}$$

$$\sum_{i \in R} \sum_{k \in K} y_i^k \leq U, \tag{23}$$

$$\sum_{b \in B} d^b \Big(\sum_{j \in \widetilde{FS}(b)} \overline{x_{bj}} (ET_{trans}^{Bio}) + \sum_{(i,j) \in R} \overline{z_{ij}^b} (ET_{trans}^{rel}) + \sum_{j \in \widetilde{RS}(s)} \overline{f_{js}^b} (ER_{rec}^{sink}) \Big) \leq \gamma, \forall\, d \in \mathcal{U}_d, \tag{24}$$

$$\sum_{i \in \widetilde{FS}(b)} \overline{x_{bi}} = 1, \qquad \forall b \in B, \tag{25}$$

$$\sum_{j \in FS(i)} \overline{z_{ij}^b} - \sum_{h \in RS(i)} \overline{z_{hi}^b} = \overline{x_{bi}} - \overline{f_{is}^b}, \qquad \forall b \in B, i \in R, \tag{26}$$

$$\overline{x_{bi}} \leq \sum_{k \in K} y_i^k a_{bi}, \qquad \forall b \in B, i \in R, \tag{27}$$

$$x_{is} \leq \sum_{k \in K} y_i^k e_{is}, \qquad \forall i \in R, \tag{28}$$

$$\sum_{i \in \widetilde{RS}(s)} x_{is} \leq g, \tag{29}$$

$$\overline{f_{is}^b} \leq x_{is} e_{is}, \quad \forall b \in B, i \in R, \tag{30}$$

$$\sum_{b \in B} \sum_{h \in RS(i)} d^b \overline{z_{hi}^b} + \sum_{b \in B} d^b \overline{x_{bi}} \leq \sum_{k \in K} v_i^k y_i^k, \qquad \forall i \in R, d \in \mathcal{U}_d, \tag{31}$$

$$\overline{x_{bi}}, \overline{z_{ij}^b}, \overline{f_{is}^b} \in \{0, 1\}. \tag{32}$$

In this model, uncertainty is incorporated into constraints (24) and (31). We can now describe the Robust Counterpart of these constraints which is obtained by utilizing the uncertainty sets defined in (16) and (19), as demonstrated in the following theorems.

Theorem 5.1. *The robust counterpart of constraints (24) and (31) with uncertain demand, given by polyhedral sets in (16), can be expressed as follows:*

$$\sum_{b \in B} \overline{d^b} \Big(\sum_{j \in \widetilde{FS}(b)} \overline{x_{bj}} (ET_{trans}^{Bio}) + \sum_{(i,j) \in R} \overline{z_{ij}^b} (ET_{trans}^{rel}) + \sum_{j \in \widetilde{RS}(s)} \overline{f_{js}^b} (ER_{rec}^{sink}) \Big) + \pi w \leq \gamma,$$

$$L^{bT} \pi \geq \rho_{d^b} \Big(\sum_{j \in \widetilde{FS}(b)} \overline{x_{bj}} (ET_{trans}^{Bio}) + \sum_{(i,j) \in R} \overline{z_{ij}^b} (ET_{trans}^{rel}) + \sum_{j \in \widetilde{RS}(s)} \overline{f_{js}^b} (ER_{rec}^{sink}) \Big) \qquad \forall b \in B,$$

$$\sum_{b\in B}\overline{d^b}(\sum_{h\in RS(i)}\overline{z^b_{hi}}+\overline{x_{bi}})+\gamma_i w\leq\sum_{k\in K}v^k_i y^k_i, \qquad \forall i\in R,$$
$$L^{bT}\gamma_i\geq\rho_b\big(\sum_{h\in RS(i)}\overline{z^b_{hi}}+\overline{x_{bi}}\big) \qquad \forall b\in B, i\in R,$$
$$\pi\geq 0,$$
$$\gamma_i\geq 0, \qquad \forall i\in R.$$

Proof. A solution to constraint (24) is referred to as robust with respect to polyhedral sets in (16). The worst-case scenario is obtained by solving the following problem:

$$\max_{\hat{d}}\sum_{b\in B}(\overline{d^b}+\rho_{d^b}\hat{d}^b)\big(\sum_{j\in\widetilde{FS}(b)}\overline{x_{bj}}(ET^{Bio}_{trans})+\sum_{(i,j)\in R}\overline{z^b_{ij}}(ET^{rel}_{trans})+\sum_{j\in\widetilde{RS}(s)}\overline{f^b_{js}}(ER^{sink}_{rec})\big)$$
$$s.t.\ \sum_{b\in B}L^b\hat{d}^b\leq w,$$
$$\hat{d}^b\geq 0, \qquad \forall b\in B.$$

The linear programming optimization problem under a polyhedral feasible region is equivalent to its dual optimization problem according to duality theory [Bertsimas and Tsitsiklis, 1997, Bazaraa et al., 2010]. Then, the dual of this problem also provides the worst-case value, as expressed by the following equation:

$$\min_{\pi}\sum_{b\in B}\overline{d^b}\big(\sum_{j\in\widetilde{FS}(b)}\overline{x_{bj}}(ET^{Bio}_{trans})+\sum_{(i,j)\in R}\overline{z^b_{ij}}(ET^{rel}_{trans})+\sum_{j\in\widetilde{RS}(s)}\overline{f^b_{js}}(ER^{sink}_{rec})\big)+\pi w$$
$$s.t.$$
$$L^{bT}\pi\geq\rho_{d^b}\big(\sum_{j\in\widetilde{FS}(b)}\overline{x_{bj}}(ET^{Bio}_{trans})+\sum_{(i,j)\in R}\overline{z^b_{ij}}(ET^{rel}_{trans})+\sum_{j\in\widetilde{RS}(s)}\overline{f^b_{js}}(ER^{sink}_{rec})\big) \qquad \forall b\in B$$
$$\pi\geq 0.$$

Similarly, the worst-case scenario of constraint (31) for each relay i can be found by addressing the following problem:

$$\max_{\hat{d}}\sum_{b\in B}\sum_{h\in RS(i)}(\overline{d^b}+\rho_{d^b}\hat{d}^b)\overline{z^b_{hi}}+\sum_{b\in B}(\overline{d^b}+\rho_{d^b}\hat{d}^b)\overline{x_{bi}}$$
$$s.t.\ \sum_{b\in B}L^b\hat{d}^b\leq w,$$
$$\hat{d}^b\geq 0, \qquad \forall b\in B.$$

The dual form of constraint (31) for every relay i, which also provides the maximum value in the worst case with dual variable γ_i, can be described as follows:

$$\min_{\gamma_i}\sum_{b\in B}\overline{d^b}(\sum_{h\in RS(i)}\overline{z^b_{hi}}+\overline{x_{bi}})+\gamma_i w$$
$$s.t.$$
$$L^{bT}\gamma_i\geq\rho_b\sum_{h\in RS(i)}\overline{z^b_{hi}}+\overline{x_{bi}} \qquad \forall b\in B$$
$$\gamma_i\geq 0.$$

Any feasible solution that satisfies the duality conditions produces an objective value that acts as a lower bound for the optimal (worst-case) value. Thus, the theorem is proven.

□

In the following theorem, we present results for an uncertain set as described in (19), which closely approximates an uncertain demand set that is spherical in shape. This set representation is suitable when all demands consist of independent normal random variables.
It is essential to highlight a crucial distinction between the uncertainty set described in set (19) and the one in (16). While the terms defining the uncertainty set in (16) are linear inequality relationships, the terms in set (19) are nonlinear. This nonlinearity introduces a significant difference in the complexity and handling of the uncertainty set. Therefore, in the upcoming theorem, our approach will involve first linearizing the nonlinear terms to facilitate the analysis, similar to the methodology employed previously. By addressing this distinction and the subsequent linearization process, we aim to enhance the understanding and treatment of the uncertainty set in (19) within the robust optimization framework.

Theorem 5.2. *The robust versions of constraints* (24) *and* (31) *with an uncertain set in* (19) *can be formulated as follows:*

$$\begin{aligned}
&\sum_{b\in B}\overline{d^b}\Big(\sum_{j\in\widetilde{FS}(b)}\overline{x_{bj}}(ET^{Bio}_{trans})+\sum_{(i,j)\in R}\overline{z^b_{ij}}(ET^{rel}_{trans})+\sum_{j\in\widetilde{RS}(s)}\overline{f^b_{js}}(ER^{sink}_{rec})\Big)+\kappa_1\theta+\sum_{b\in B}\kappa_\infty(\eta^{b+}+\eta^{b-})\le\gamma\\
&\theta+\eta^{b+}\ge\rho_{d^b}\Big(\sum_{j\in\widetilde{FS}(b)}\overline{x_{bj}}(ET^{Bio}_{trans})+\sum_{(i,j)\in R}\overline{z^b_{ij}}(ET^{rel}_{trans})+\sum_{j\in\widetilde{RS}(s)}\overline{f^b_{js}}(ER^{sink}_{rec})\Big),\quad\forall b\in B\\
&\theta+\eta^{b-}\ge-\rho_{d^b}\Big(\sum_{j\in\widetilde{FS}(b)}\overline{x_{bj}}(ET^{Bio}_{trans})+\sum_{(i,j)\in R}\overline{z^b_{ij}}(ET^{rel}_{trans})+\sum_{j\in\widetilde{RS}(s)}\overline{f^b_{js}}(ER^{sink}_{rec})\Big),\quad\forall b\in B,\\
&\sum_{b\in B}\overline{d^b}\Big(\sum_{h\in RS(i)}\overline{z^b_{hi}}+\overline{x_{bi}}\Big)+\kappa_1\alpha_i+\sum_{b\in B}\kappa_\infty(\beta_i^{b+}+\beta_i^{b-})\le\sum_{k\in K}v_i^k y_i^k,\quad\forall i\in R,\\
&\alpha_i+\beta_i^{b+}\ge\rho_b\Big(\sum_{h\in RS(i)}\overline{z^b_{hi}}+\overline{x_{bi}}\Big),\quad\forall b\in B, i\in R,\\
&\alpha_i+\beta_i^{b-}\ge-\rho_b\Big(\sum_{h\in RS(i)}\overline{z^b_{hi}}+\overline{x_{bi}}\Big),\quad\forall b\in B, i\in R,\\
&\theta,\eta^{b+},\eta^{b-},\alpha_i,\beta_i^{b+},\beta_i^{b-}\ge 0,\quad\forall b\in B, i\in R.
\end{aligned}$$

Proof. The worst-case scenario of constraint (24) concerning the uncertain set in (19) can be identified by addressing the following problem:

$$\begin{aligned}
&\max_{\hat d}\sum_{b\in B}(\overline{d^b}+\rho_{d^b}\hat{d^b})\Big(\sum_{j\in\widetilde{FS}(b)}\overline{x_{bj}}(ET^{Bio}_{trans})+\sum_{(i,j)\in R}\overline{z^b_{ij}}(ET^{rel}_{trans})+\sum_{j\in\widetilde{RS}(s)}\overline{f^b_{js}}(ER^{sink}_{rec})\Big)\\
&s.t.\ \sum_{b\in B}|\hat{d^b}|\le\kappa_1,\\
&|\hat{d^b}|\le\kappa_\infty,\ \forall b\in B.
\end{aligned}$$

or we can also write

$$\begin{aligned}
&\max_{\hat d}\sum_{b\in B}(\overline{d^b}+\rho_{d^b}(d^{\hat b+}-d^{\hat b}-))\Big(\sum_{j\in\widetilde{FS}(b)}\overline{x_{bj}}(ET^{Bio}_{trans})+\sum_{(i,j)\in R}\overline{z^b_{ij}}(ET^{rel}_{trans})+\sum_{j\in\widetilde{RS}(s)}\overline{f^b_{js}}(ER^{sink}_{rec})\Big)\\
&s.t.\ \sum_{b\in B}d^{\hat b+}+d^{\hat b}-\le\kappa_1,\\
&0\le d^{\hat b+}\le\kappa_\infty,\ \forall b\in B,\\
&0\le d^{\hat b-}\le\kappa_\infty,\ \forall b\in B.
\end{aligned}$$

This problem's dual also yields the worst-case value. The dual is written as

Biosensor	A	B	C	D	E	F	G	H	I	J	K	L	M	sink
x-coordinate (m)	0.10	-0.20	-0.03	0.05	0.10	-0.10	-0.10	0.10	-0.10	-0.05	0	0.20	0.10	0
y-coordinate (m)	-0.60	-0.10	0.10	0.25	-0.90	-0.30	0.35	0.35	0.60	0	0.70	-0.20	0.90	0
Single-hop (m)	0.66	0.13	0.14	0.47	0.85	0.23	0.53	0.53	0.66	0.3	0.8	0.31	0.85	-
Multi-hop (m)	0.66	0.13	0.14	0.47	0.2	0.17	0.36	0.07	0.45	0.48	0.37	0.58	0.2	-

Table 2
Deployment of biosensors on patient's body. Distances (in meters) between biosensors and the sink for the single-hop case, and between biosensors and the nearest node for the multi-hop case.

$$\min_{\theta,\eta^+,\eta^+} \sum_{b\in B} \overline{d^b}\Big(\sum_{j\in \widetilde{FS}(b)} \overline{x_{bj}}(ET^{Bio}_{trans}) + \sum_{(i,j)\in R} \overline{z^b_{ij}}(ET^{rel}_{trans}) + \sum_{j\in \widetilde{RS}(s)} \overline{f^b_{js}}(ER^{sink}_{rec})\Big) + \kappa_1\theta + \sum_{b\in B}\kappa_\infty(\eta^{b+}+\eta^{b-})$$

$$s.t. \theta + \eta^{b+} \geq \rho_{d^b}\Big(\sum_{j\in \widetilde{FS}(b)} \overline{x_{bj}}(ET^{Bio}_{trans}) + \sum_{(i,j)\in R} \overline{z^b_{ij}}(ET^{rel}_{trans}) + \sum_{j\in \widetilde{RS}(s)} \overline{f^b_{js}}(ER^{sink}_{rec})\Big), \quad \forall b \in B$$

$$\theta + \eta^{b-} \geq -\rho_{d^b}\Big(\sum_{j\in \widetilde{FS}(b)} \overline{x_{bj}}(ET^{Bio}_{trans}) + \sum_{(i,j)\in R} \overline{z^b_{ij}}(ET^{rel}_{trans}) + \sum_{j\in \widetilde{RS}(s)} \overline{f^b_{js}}(ER^{sink}_{rec})\Big), \quad \forall b \in B.$$

The worst-case scenario for constraint (31) for each relay i can be determined by solving the following problem:

$$\max_{\hat{d}} \sum_{b\in B}\sum_{h\in RS(i)} (\overline{d^b} + \rho_{d^b}(d^{\hat{b}+} - d^{\hat{b}}-))\overline{z^b_{hi}} + \sum_{b\in B}(\overline{d^b} + \rho_{d^b}(d^{\hat{b}+} - d^{\hat{b}}-))\overline{x_{bi}}$$

$$s.t. \sum_{b\in B} d^{\hat{b}+} + d^{\hat{b}}- \leq \kappa_1,$$

$$0 \leq d^{\hat{b}+} \leq \kappa_\infty, \forall b \in B,$$

$$0 \leq d^{\hat{b}-} \leq \kappa_\infty, \forall b \in B.$$

By assigning the dual variables α_i, β_i^{b+}, and β_i^{b-} to the dual form of the above formulation for each relay i, we can achieve the result. Therefore, the theorem is proven.

□

The models introduced in this paper involve constraints that must be satisfied for all traffic vectors d within the uncertainty set, $d \in \mathcal{U}_d$. When $\mathcal{U}_d$ takes the form of a polytope with a polynomial number of extreme points, some formulations such as those concerning dynamic WBAN design can be effectively solved by considering the constraints related to each extreme point. However, for most of the polytopes considered in the literature (such as those described above), the number of extreme points is not polynomial. In such cases, there are primarily two methods to handle constraints involving d: either employing cutting-plane algorithms where traffic vectors are generated in an iterative way [Ben-Ameur and Kerivin, 2003], or adopting duality-based approaches [Ben-Tal et al., 2009a]. While the cutting-plane approach can be applied to any tractable polytope (i.e., for which separation is polynomial), the latter method is recommended when the polyhedral set can be described using a limited number of variables and constraints [Ben-Ameur et al., 2011, Ben-Tal et al., 2009a].

6. Wireless Body Area Network Scenario

In this section, we present the topology and scenario of the wireless body area network considered in our numerical evaluation. The topology consists of a set of 13 biosensors of various types, strategically placed on specific parts of the body to monitor and transfer data to the sink device. Virtual 2D coordinates (x,y) specify network components location, as detailed in Table 2. Referring to Figure 5, the sink device is positioned at the origin of the coordinate system, and ensures accessibility to all devices. The Euclidean distance between each biosensor and its nearest node, in multi-hop communication, is also reported in Table 2. Additionally, eight ellipsoidal regions, shown in Figure 5, have been identified for installing relays uniformly at random on the body surface or patient's clothes. These regions

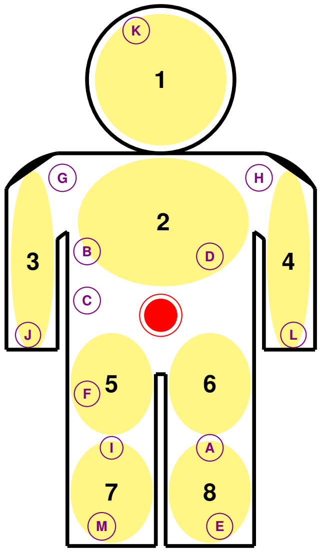

Figure 5: A wireless body area network with different areas for installing relays.

cover the entire body surface, ensuring that transferring data through multi-hop communication is not affected by changes in body state or network topology. In other words, these regions have been carefully selected to facilitate communication between devices and ensure that body movements do not interfere with the monitoring process. The topology is designed for healthcare applications and represents a normal *standing* scenario with arms hanging on the sides. For each experiment, described in the next Section, the maximum number of relays that can be installed (candidate sites, U) is assumed to be 80, but only a few are actually installed as we will detail in the next Section.

Wireless nodes in a WBAN access the channel through various wireless technologies and protocols tailored for healthcare monitoring applications, typically requiring low power consumption (often less than 1 mW peak power) within short communication distances, usually up to 2 meters [Zhong et al., 2022]. WBANs utilize wireless standards like Bluetooth, Zigbee, WiFi, and IEEE 802.15.6 to enable communication among wearable and implantable sensors [Latré et al., 2011, Arefin et al., 2017]. Channel access methods in WBANs involve techniques such as Contention-Based Access with Collision Avoidance (CSMA/CA) and Slotted ALOHA to manage channel access efficiently [Arefin et al., 2017, Zhong et al., 2022]. However, WBANs face challenges such as intra-BAN interference, mitigated using Time Division Multiple Access (TDMA) techniques, while inter-WBAN interference may occur when multiple WBANs are co-located. The control system manages the network, providing TDMA cycle parameter values for equal distribution of TDMA device slots among nodes [Mohanty et al., 2023]. In this work, we focus on the routing level, assuming the adoption of solutions proposed at the MAC/physical layer for successful and reliable communication of biosensors [Arefin et al., 2017, Zhong et al., 2022, Mohanty et al., 2023] at such layers to ensure successful/reliable communication of biosensors. To ensure optimal healthcare services, minimize heat absorption by devices [Elias, 2014, Zhou et al., 2017, Shahbazi and Byun, 2020], prevent signal interference [Samal et al., 2019], and reduce network energy consumption [Shahbazi and Byun, 2020], it is crucial to limit the communication range of devices and reduce transmission power. Given that wireless communication takes place in close proximity to the human body, it is important to consider Specific Absorption Rates (SAR), which measure the amount of radio frequency energy absorbed by human tissue per unit mass [Wu and Lin, 2014]. As the distance between biosensors and the sink increases, higher transmission power is required to ensure packet delivery, which can lead to increased heat and SAR levels. To mitigate these risks, we have employed intermediate relay nodes to adjust the distance between biosensors and the sink, allowing for low transmission power and ensuring that SAR levels remain within acceptable thresholds. Our topology is carefully designed to facilitate communication between devices while minimizing the potential risks associated with wireless communications near the human body.

Multi-hop communication has the potential to mitigate the adverse effects of SAR while simultaneously improving transmission success rates [Wu and Lin, 2014, Ahmed et al., 2018]. To regulate the distance between network components, we assign connectivity parameters a_{bi} and e_{is} a value of 1 only if a relay i is installed within a radius

Parameter	Value
E_{TXelec}	16.7 (nJ/bit)
E_{RXelec}	36.1 (nJ/bit)
$E_{amp}(3.38)$	1.97 (nJ/bit)
$E_{amp}(5.9)$	7990 (nJ/bit)
Frequency range	2.4 – 2.45 GHz

Table 3
Energy consumption values and frequency range for the Nordic nRF2401 transceiver.

no greater than the defined communication range (CR) in centimeters for both biosensors and the sink, respectively. In wireless channel propagation models, the path loss power is typically assumed to be 2 for free space propagation and around 4 in lossy environments. However, the path loss power can exceed 4 when transmission occurs around the human body, with values ranging from 5 to 7.4 [Elias, 2014]. Specifically, line-of-sight transmission typically has a propagation value of about 3.38, whereas non-line-of-sight transmission around the body has a propagation value of approximately 5.9. For the computation of the network energy consumption, we utilize parameters specific to the Nordic nrf2401 transceiver, which operates within the 2.4-2.45 GHz frequency range and is commonly employed in wireless body networks [Kaur et al., 2021, Elias, 2014, Reusens et al., 2009]. These parameters are detailed in Table 3. Therefore, the initial parameters for assessing network energy consumption in both deterministic and robust models are E_{TXelec} and E_{RXelec}, which correspond to transmitter and receiver circuitry, respectively. Furthermore, to regulate the communication distance between devices and minimize the required transmission power, we incorporated amplifier energy to sustain weak signals until routing completion and efficiently manage their transmission to the subsequent device in the communication path. Consequently, the amplifier energy, which is dependent on path loss value, for line-of-sight (LOS) transmission ($n = 3.38$) and non-line-of-sight (NLOS) transmission ($n = 5.9$) was calculated as $Eamp(3.38) = 1.97$ (nJ/bit) and $Eamp(5.9) = 7990$ (nJ/bit), respectively.

7. Numerical Results

In this section we will discuss the computational experiments that compare *Robust* solutions to *Deterministic* ones; these latter are obtained by replacing d in the LOU model (15) with its nominal or average data rate $\overline{d}$. We utilize two data uncertainty sets, specifically *polyhedral* and *intersection*, defined in (16) and (19), respectively. Our set of experiments aims to demonstrate that the robust approach is more suitable for WBANs than the deterministic ones since biosensors may generate an uncertain amount of data, even though in a given range.

Before presenting the metrics used to evaluate the performance of our proposed approach, we emphasize that our work is compared against two baseline approaches:

- **Deterministic Model:** This model assumes perfect knowledge of the problem parameters without any consideration of uncertainty. While it provides a benchmark for ideal conditions, it lacks the robustness needed to handle real-world variability.
- **Worst Case Scenario:** This approach accounts for uncertainty by considering the most adverse conditions within the uncertainty set. It is comparable to the robust optimization model proposed by D'Andreagiovanni et al. [D'Andreagiovanni and Nardin, 2015], which minimizes the maximum deviation between proposed and optimal solutions across all scenarios. However, as discussed before, our two-stage robust approach offers greater flexibility than the single-stage model of D'Andreagiovanni et al., enabling more adaptable and efficient solutions.

To assess the effectiveness of our methodology relative to these baselines, we use the following four metrics:

- Z_D: the optimal value of deterministic solutions.
- Z_R: the conservative estimate of the optimal value obtained by solving the two-stage robust problem under uncertain data parameters. Z_R can be compared with Z_D to assess the impact of uncertainty on the performance of the network. If Z_R is higher but close to Z_D, it means that the solution is robust to uncertainty, that is, the network can overcome the worst-case scenario.

- Z_{WC}: the worst-case value of the deterministic solution when data rate is subject to uncertainty. Therefore, it measures the maximum (i.e., worst) possible output value that can be obtained from the model under all possible scenarios involving uncertain data.
- Z_{AC}: the objective function's value of the robust solution under the deterministic scenario. In other words, Z_{AC} measures the performance of the solution obtained from a robust optimization problem when the input data is known with certainty. This metric provides a measure of how well the robust solution performs under ideal conditions, when there is no uncertainty in the input data.

Finally, in each experiment, we compare the performance of robust and deterministic solutions using the following two metrics:

$$R_{WC} = \frac{Z_{WC} - Z_R}{Z_R}, \qquad R_{AC} = \frac{Z_{AC} - Z_D}{Z_D}.$$

Specifically, metric R_{WC} measures the relative improvement of the robust solution in the worst case and R_{AC} is the relative loss of optimality of the robust solution on the nominal data.

7.1. Experiment 1: Performance metrics and Relay Capacity analysis with Polyhedral uncertainty

In this first set of experiments, we assume that the generated data d are within the Polyhedral uncertainty set:

$$\text{Polyhedral:} \qquad \mathcal{U}_d = \left\{ d \in \mathcal{R}^{|B|} | d = 80 + \rho_d \hat{d},\ \sum_{b \in B} \hat{d}^b \leq w = 50, \hat{d} \geq 0 \right\}.$$

Figure 6 reports the trend of metrics Z_D, Z_R, Z_{WC} and Z_{AC} as a function of the uncertainty level $\rho_d \in [0, 1]$ with 0.1 increments. Initially, there is almost no change in all metrics while ρ_d increases from 0 to 0.3; then, the changes are more evident starting at $\rho_d = 0.3$. According to the figure, there exists, at most, a 12.7% gap between Z_D and Z_R; specifically, this gap raises as ρ_d grows, and assumes values from 0 to 12.7%. Thus, the robust solution only deviates slightly from the optimal solution when using deterministic data parameters.

In contrast to the robust model optimal value, Z_{WC} sharply jumps as the uncertainty level raises from 0.3 to 0.8, then this metric gradually increases and stabilizes for $\rho_d \geq 0.8$. In fact, as the uncertainty levels increase, the worst-case value of the deterministic solution increases too because it requires the installation of relay nodes with higher capacity and therefore a higher investment cost.

In Figure 7, we illustrate R_{AC} and R_{WC} versus ρ_d within the $[0, 1]$ range for $w = 50$ (refer to equation 16, reported at the beginning of this subsection for sake of clarity) to evaluate the effectiveness of the robust solution in reducing worst-case energy consumption and the level of optimality lost in the deterministic model due to the robust solution. It is important to note that implementing a WBAN using the suggested two-stage robust approach results in only a 6.4% increase in energy consumption compared to the deterministic approach. However, it is crucial to consider worst-case scenarios, as evidenced by the plateau observed in the R_{AC} curve. In contrast, developing a WBAN without considering data uncertainty could result in worst-case scenarios, leading to a significant loss in energy resources (24%) per data transmission, as depicted by the R_{WC} curve. This highlights that the energy consumption rise in the robust approach is significantly lower than that in the worst-case scenario, meaning that the robust WBAN design can flexibly handle data uncertainty considering the actual design of such networks, while adopting a conservative approach to data transmission.

Relay Capacity Analysis

The emergence of uncertainty in the network necessitates changes in its topology. This is especially true when the level of uncertainty increases. In fact, the decision-making regarding the *number* of relays to install and the selection of their capacities is a major challenge in the context of wireless body area network design. Moreover, relays' capacities should be chosen in a way that, in addition to guaranteeing low installation costs, they provide sufficient capacity for data transmission even when the worst-case data rates occur.

Figures 8-10 illustrate the distribution of the installed relays with four different capacity values, denoted as $v^k, k \in K$, where $v^1 < v^2 < v^3 < v^4$. These values are randomly extracted from a uniform distribution between 100 to 400. We observe, however, that similar results (not shown for sake of brevity) were obtained fixing capacity values

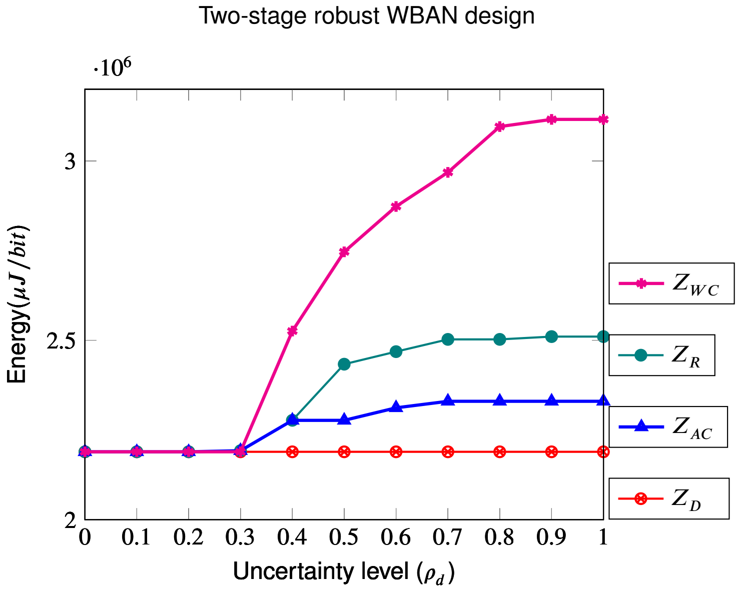

Figure 6: Comparison of Z_D, Z_R, ,Z_{AC} and Z_{WC} as a function of the uncertainty level $\rho_d \in [0, 1]$.

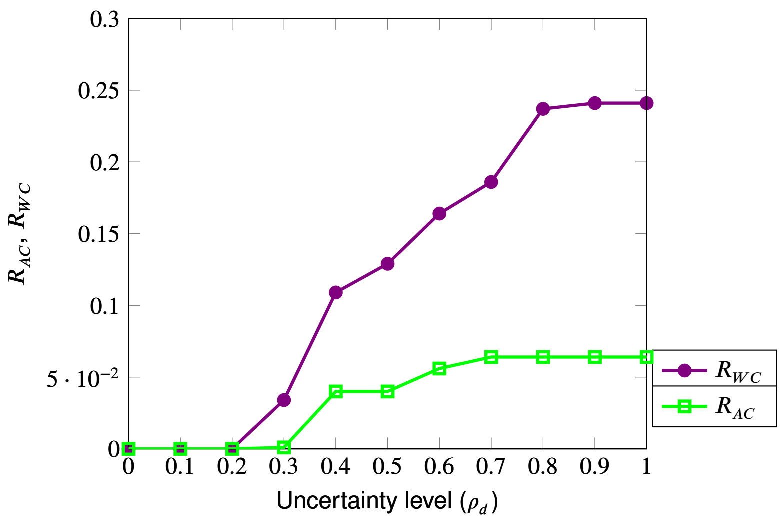

Figure 7: Comparison of R_{AC} and R_{WC} as a function of the uncertainty level $\rho_d \in [0, 1]$.

to 100, 200, 300 and 400 for v^1, v^2, v^3 and v^4 respectively. Similarly, the investment/relay installation costs, which increase proportionally to relay capacities' values, range uniformly from 120 to 700 monetary units. Constraint (12) imposes that only one relay of capacity type k can be installed at each candidate site i.

The comparison is made between the MIP model with nominal data rate $(\overline{d^b})$, the two-stage robust model considering uncertain data within a polyhedral uncertainty set, and the worst-case scenario, with ρ_b varying in the set $\{0.3, 0.6, 0.9\}$.

Figure 8 illustrates that in the deterministic model, 28.6% and 42.9% of relays were installed with the lowest capacity (v^1 and v^2, respectively), and 28.5% were installed with capacity v^3. However, the pattern changes when we introduce uncertainty. With an uncertainty level $\rho_b = 0.3$, in the proposed robust model, 71.3% of the relays are installed with the lowest capacities of type v^1 (14.3%) and v^2 (57%), while almost 60% of the installed relays in the worst-case scenario have the highest capacities: v^3 (42.9%) and v^4 (14.3%).

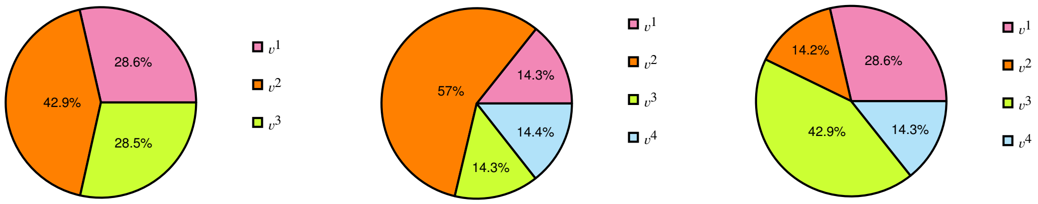

(a) Deterministic model (b) Two-stage robust model (c) Worst-case scenario

Figure 8: Percentage of installed relays with capacities υ^1, υ^2, υ^3, and υ^4 under a polyhedral uncertainty set with $\rho_b = 0.3$.

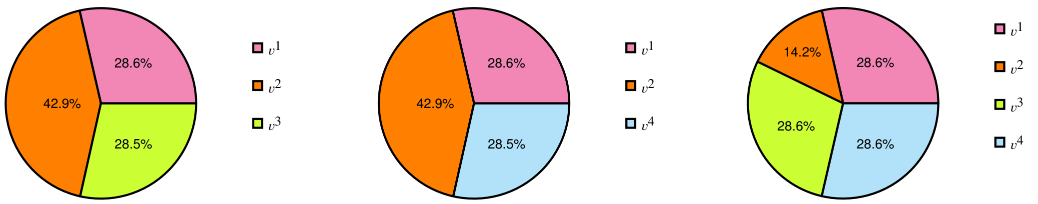

(a) Deterministic model (b) Two-stage robust model (c) Worst-case scenario

Figure 9: Percentage of installed relays with capacities υ^1, υ^2, υ^3, and υ^4 under a polyhedral uncertainty set with $\rho_b = 0.6$.

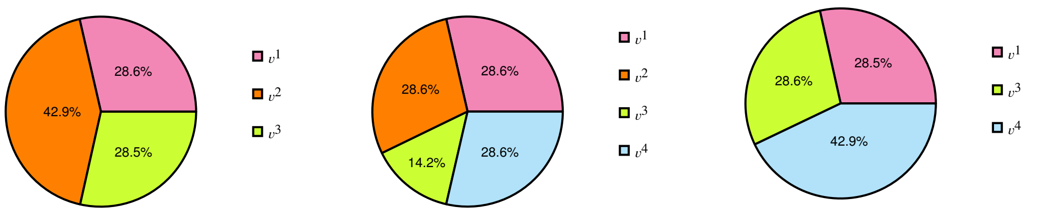

(a) Deterministic model (b) Two-stage robust model (c) Worst-case scenario

Figure 10: Percentage of installed relays with capacities υ^1, υ^2, υ^3, and υ^4 under a polyhedral uncertainty set with $\rho_b = 0.9$.

Figure 9 further demonstrates that the robust approach offers high flexibility and exhibits a behavior closely resembling that of the deterministic model, even when the uncertainty level increases to $\rho_b = 0.6$; in fact, with such a ρ_b value, the robust model installs a total of 71% relays of type υ^1 (28.6%) and υ^2 (42.9%). Furthermore, it only installs relays of type υ^4 (28.5%, and none of type υ^3) as compared to the case where $\rho_b = 0.3$ (14.4% of type υ^4 and 14.3% of type υ^3) to accommodate the increasing network traffic.

In this scenario, the worst-case model shows more variety in installing relays. This provides a topology for the network in which 28.6% of the relays have type 1 capacity, 14.2% of the relays have capacity υ_2, 28.6% υ_3, and finally, 28.6% of the relays have the highest installed capacity. Finally, Figure 10 illustrates that more than 71.5% of the total number of relays are installed with high capacity in the worst-case scenario model when $\rho_b = 0.9$ (28.6% of type υ^3 and 42.9% of type υ^4), while in the robust model, about 43% of the relays were installed with such capacities (υ^3 and υ^4).

Hence, to summarize, the deterministic model does not account for variability and uncertainty in data rates, which is critical in practical scenarios where data traffic can be highly unpredictable. This inflexibility can result, especially when data rate uncertainty increases, in either under-provisioning (leading to failures in data transmission and hence in patients monitoring) or over-provisioning (leading to unnecessary costs); installing a large number of relays with high capacity would in fact significantly increase costs for patients, thus violating the principle of provisioning cheap health services, which is one of the goals of WBANs.

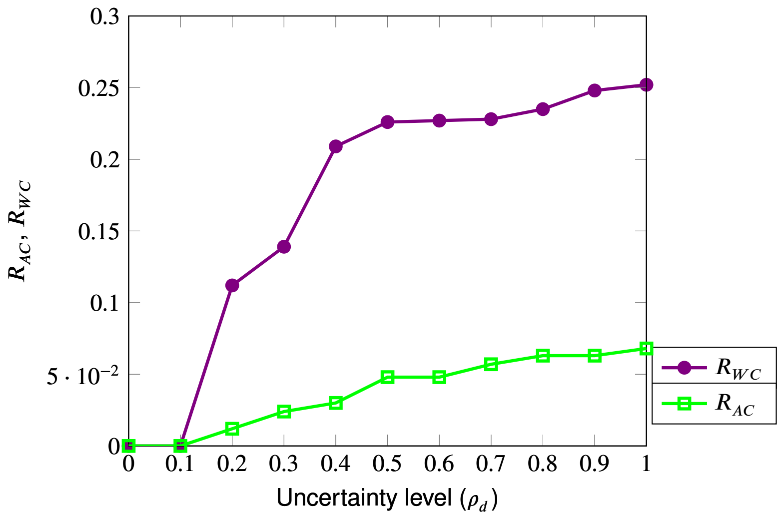

Figure 11: Comparison of the mean of R_{AC} and R_{WC} as a function of the uncertainty level $\rho_d \in [0, 1]$ in increments of 0.1 with respect to w.

In contrast to the worst-case scenario, our two-stage robust WBAN design model selects relay capacities while considering a range of potential data rate scenarios within an uncertainty set in the first stage. This stage offers a solution that remains feasible under various potential data rate realizations, with 71.3% and 71% of the relays being equipped with the lowest capacity for $\rho_b = 0.3$ and $\rho_b = 0.6$, respectively. Even at the highest uncertainty level of $\rho_b = 0.9$, this percentage remains at 57.2%.

At this stage we reconsider the Polyhedral uncertainty set $\mathcal{U}_d = \left\{ d \in \mathcal{R}^{|B|} | d = 80 + \rho_d \hat{d}, \sum_{b \in B} \hat{d}^b \leq w, \hat{d} \geq 0 \right\}$, and we vary the parameter w's value in the set $\{50, 100, 150, 200, 250, 300\}$.

Figure 11 compares the average value (with respect to w) of ratios R_{AC} and R_{WC} as a function of the uncertainty level $\rho_d \in [0, 1]$.

The results indicate that the robust solution is only slightly suboptimal for the deterministic data parameters, while it significantly reduces the worst-case cost, especially when the uncertainty level in data rates increases.

7.2. Experiment 2: Performance metrics and Relay Capacity analysis with Intersection uncertainty

In this second set of experiments we assume that the generated data d fall in the following *intersection* uncertainty set:

$$\text{Intersection:} \qquad \mathcal{U}_d = \left\{ d \in \mathcal{R}^{|B|} | d = 80 + \rho_d \hat{d}, \|\hat{d}\|_\infty \leq 4, \|\hat{d}\|_1 \leq 50 \right\}$$

Figure 12 shows the metrics Z_D, Z_R, Z_{AC}, and Z_{WC} plotted against the uncertainty level $\rho_d \in [0, 1]$.

The curves in Figure 12 show that Z_{AC} and Z_R almost overlap, exhibiting minimal variance at each uncertainty level. Moreover, the maximum increase in Z_R over Z_D amounts to 26.6% as ρ_d reaches 1. Furthermore, as the uncertainty level increases, Z_{wc} can reach up to 162% of Z_D and 106% of Z_R. This suggests that adopting a robust strategy towards data variability and implementing a resilient strategy for WBANs in specific scenarios does not result in wasteful energy consumption within the network and permits to manage worst-case scenarios while decreasing network energy usage. Figure 13 illustrates the energy loss in the aforementioned scenarios through the R_{AC} and R_{WC} metrics. The R_{AC} metric shows a slight increase as ρ_d increases. In contrast, the R_{WC} metric exhibits a significant rise as the ρ_d parameter increases. The optimality loss exceeds 49% for $\rho_d > 0.5$. This implies that with an increasing uncertainty level in the data rate, energy loss also rises, underscoring the importance of considering data rate uncertainty in energy-aware WBANs to reduce energy loss while maintaining a consistent data output from biosensors.

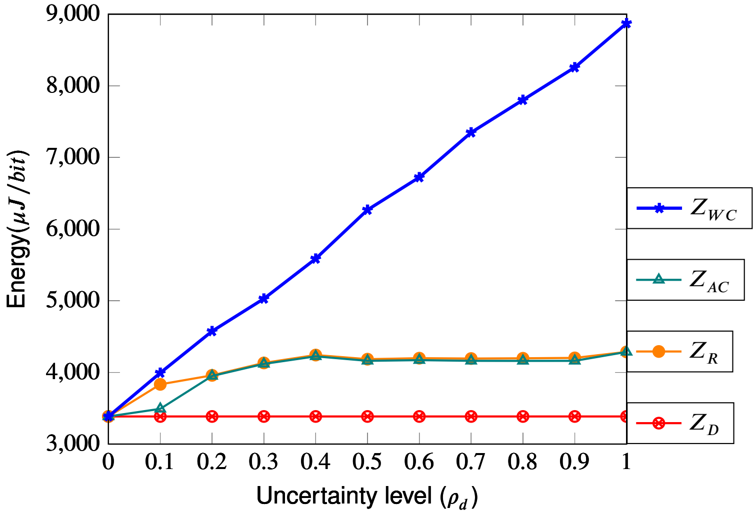

Figure 12: Intersection uncertainty set: comparison of Z_D, Z_R, ,Z_{AC} and Z_{WC} as a function of the uncertainty level $\rho_d \in [0, 1]$.

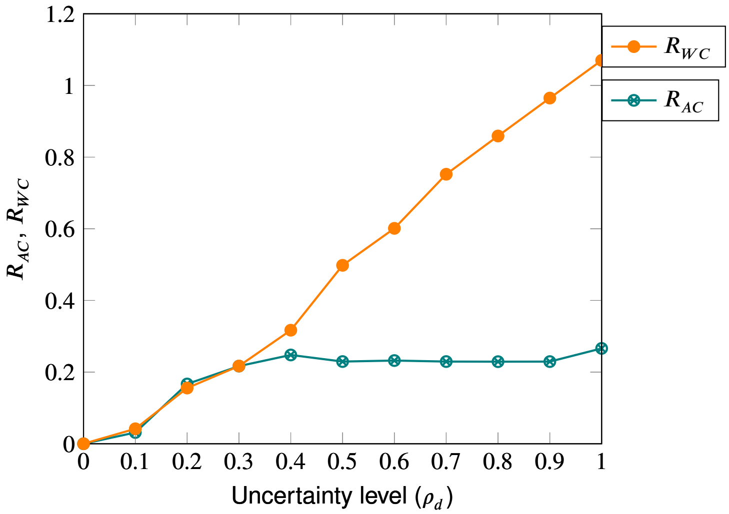

Figure 13: Comparison ofR_{AC} and R_{WC} as a function of the uncertainty level $\rho_d \in [0, 1]$ in increments of 0.1.

Relay Capacity Analysis

As previously discussed, the uncertainty in data rate presents a challenge in selecting relay capacities for wireless body area networks. Figures 14-16 show the percentage of installed relays with varying capacities, v^k, under uncertain conditions. Four capacity levels, $v^1 < v^2 < v^3 < v^4$, are considered as before for the deterministic MIP model with nominal data rate, the two-stage robust model, and the worst-case scenario under the intersection uncertainty set.

In Figure 14, the deterministic model installs no relays with maximum capacity (v^4) and 28.6% of type v^3, while 71.5% are lower capacity relays (v^1 and v^2). When uncertainty is present, even at a high level ($\rho_d = 0.9$), the two-stage robust model shows flexibility in selecting relay capacities. In Figure 14, 12.5% and 75% of relays are installed with the lowest capacities (v^1 and v^2) at $\rho_d = 0.3$. These values change slightly as uncertainty increases to $\rho_d = 0.6$

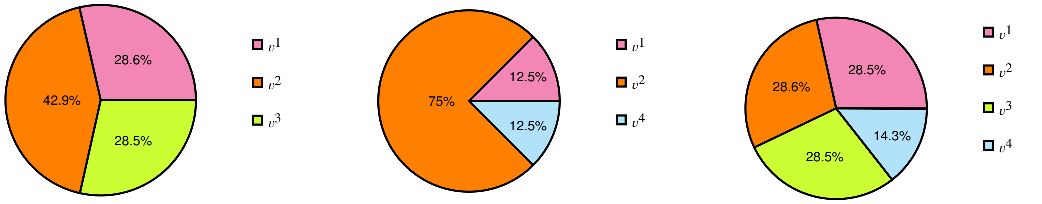

(a) Deterministic model (b) Two-stage robust model (c) Worst-case scenario

Figure 14: Percentage of installed relays with capacities υ^1, υ^2, υ^3, and υ^4 under an intersection uncertainty set with $\rho_b = 0.3$.

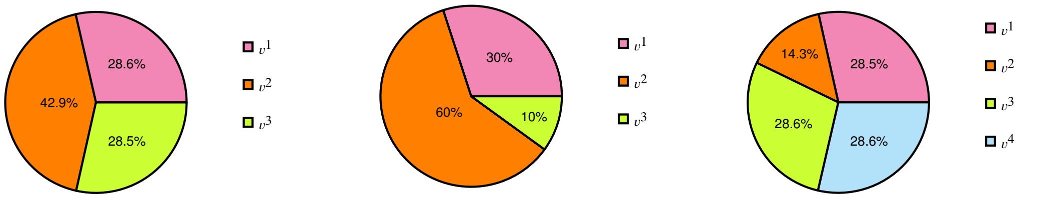

(a) Deterministic model (b) Two-stage robust model (c) Worst-case scenario

Figure 15: Percentage of installed relays with capacities υ^1, υ^2, υ^3, and υ^4 under an intersection uncertainty set with $\rho_b = 0.6$.

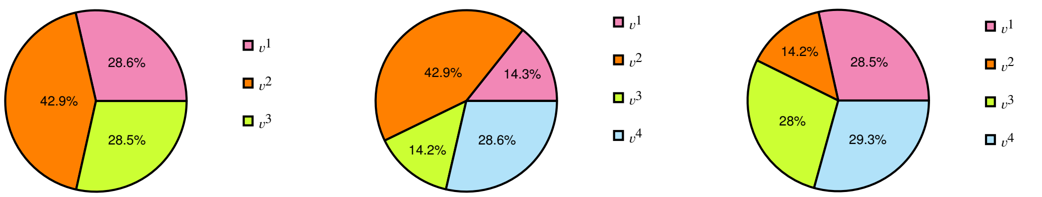

(a) Deterministic model (b) Two-stage robust model (c) Worst-case scenario

Figure 16: Percentage of installed relays with capacities υ^1, υ^2, υ^3, and υ^4 under an intersection uncertainty set with $\rho_b = 0.9$.

(Figure 15), with 30% of relays at υ^1, 60% at υ^2, and 10% at υ^3. At the highest uncertainty level ($\rho_d = 0.9$), 28.6% of relays are installed with the highest capacity (υ^4), while 57.2% are at υ^1 and υ^2 (Figure 16).

The robust model effectively selects appropriate relay capacities to ensure data transmission despite traffic uncertainty. In contrast, the worst-case scenario installs relays with the highest capacity, with about 60% of relays being υ^3 and υ^4 as uncertainty increases from 0.3 to 0.9.

Impact of uncertainty on the R_{WC} and R_{AC} metrics

This section explores how the uncertainty set impacts the metrics R_{WC} (relative improvement of the robust solution in the worst case) and R_{AC} (relative loss of optimality of the robust solution on the nominal data). Figure 17 illustrates the trend of the R_{WC} metric as a function of the uncertainty level ρ_d for the polyhedral (R_{WC}^{POL}) and the intersection uncertainty set (R_{WC}^{INT}). From Figure 17, it is evident that when the network operates under a polyhedral uncertainty set, robust solutions offer greater improvement in the worst-case scenario compared to when an intersection uncertainty set is utilized. Specifically, the metric R_{WC}^{INT} shows a sharp increase with higher uncertainty levels of ρ_d, while R_{WC}^{POL} demonstrates almost plateaued growth. Additionally, there is an 85% gap between them in terms of ratio differences.

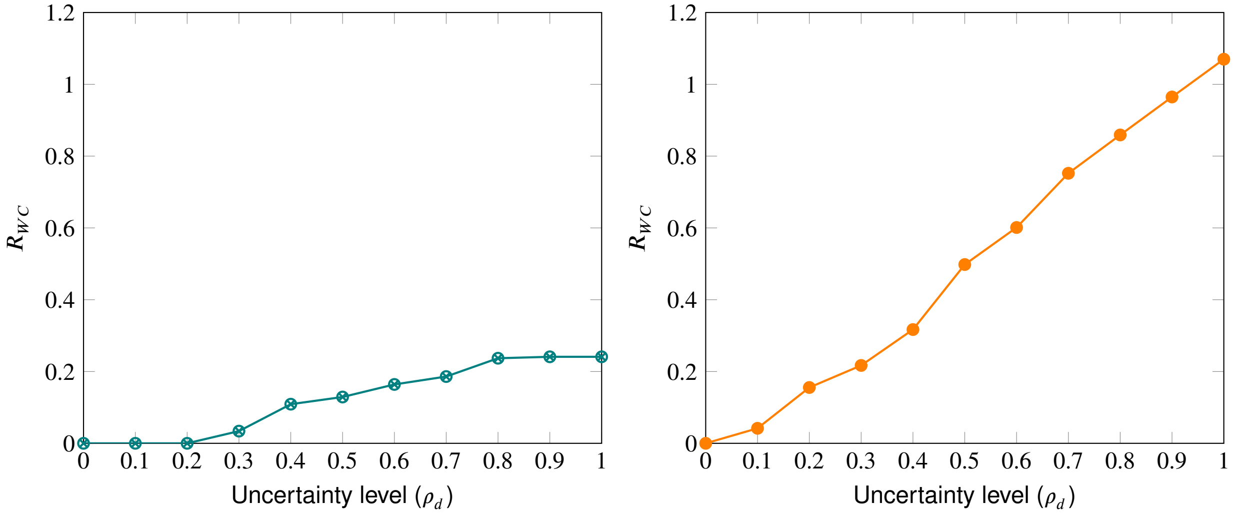

(a) Polyhedral uncertainty set (b) Intersection uncertainty set

Figure 17: Relative improvement of the robust solution in the worst case, R_{WC}, with (a) Polyhedral and (b) Intersection uncertainty set.

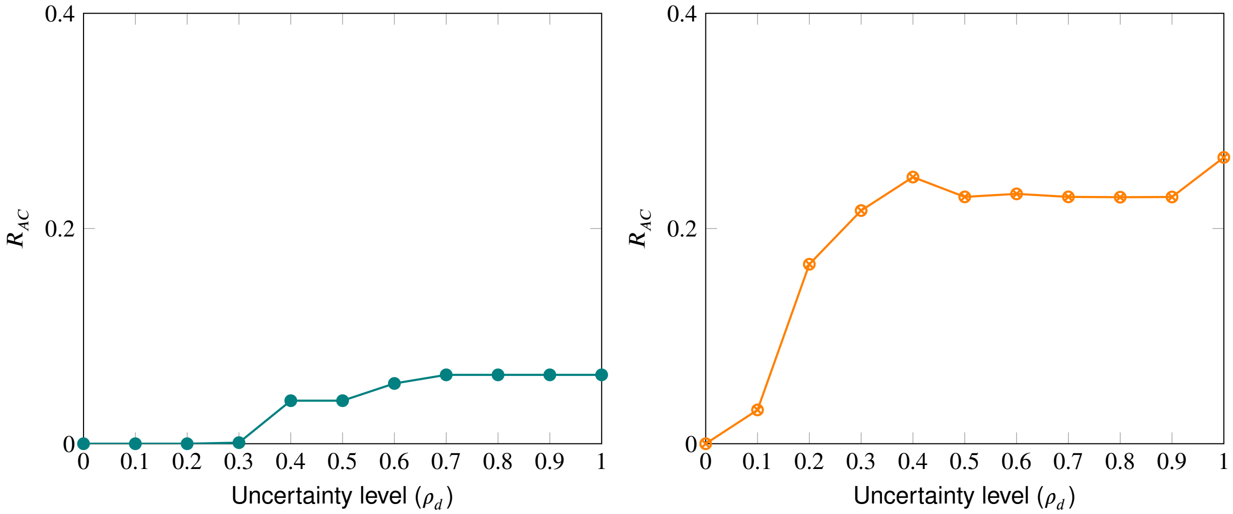

(a) Polyhedral uncertainty set (b) Intersection uncertainty set

Figure 18: Relative loss of optimality of the robust solution on the nominal data, R_{AC}, with (a) Intersection and (b) Polyhedral uncertainty set.

In Figure 18, we plot R_{AC}^{POL} and R_{AC}^{INT} to compare the energy loss percentages of robust solutions with nominal parameters. The Two-stage Robust approach under the polyhedral uncertainty set can optimize a WBAN for energy efficiency, resulting in a 6.4% increase in energy consumption for nominal parameters (as shown by the R_{AC}^{POL} curve). In contrast, the robust formulation under the intersection uncertainty set would incur a 27% energy loss under the same nominal scenario (as shown by the R_{AC}^{INT} curve).

Impact of Relay Installation Costs on Model Performance

In this section, we examine the impact of increasing relay installation costs on the performance of our two-stage robust model. We compare our model to two approaches, the MIP model with nominal data rate ($\overline{d^b}$) and the worst-case scenario, considering uncertain data within an Intersection uncertainty set. For all scenarios, we set the uncertainty level to $\rho_b = 0.6$.

We consider as before relays with four different capacity values, denoted as $\upsilon^k, k \in K$, where $\upsilon^1 < \upsilon^2 < \upsilon^3 < \upsilon^4$. These values are randomly extracted from a uniform distribution between 80 and 480 Mbps.

To model the installation costs, we implement the following concave logarithmic function that represents the complex relationship between relay capacity and cost. This mathematical approach captures the non-linear nature of cost increases in our application, providing a more realistic representation of real-world infrastructure investment scenarios.

$$C(x) = a \cdot \log(1 + bx) \tag{33}$$

where $C(x)$ is the cost, x is the relay capacity, a is a scaling factor, and b is a parameter that affects the rate of cost increase. The logarithmic function encapsulates cost modeling characteristics through its design. Costs consistently increase with capacity, reflecting the reality that larger installations require more resources. Simultaneously, the function demonstrates diminishing marginal costs, where the rate of cost increase gradually decelerates as capacity expands. This approach mirrors real-world economies of scale, where incremental capacity investments become progressively more efficient.

We set the scaling factor a to 100 initially and vary the parameter b from 10 to 30 to explore different cost scenarios. This range for b allows us to examine how the rate of cost increase affects our WBAN design and performance metrics.

We measure and show hereafter the metrics introduced before, Z_D, Z_R, Z_{WC} and Z_{AC} for the objective function values as well as R_{WC} (relative improvement of the robust solution in the worst case) and R_{AC} (relative loss of optimality of the robust solution on the nominal data).

Figure 19 illustrates a comparative analysis of the robust, deterministic, and worst-case models as the cost parameter escalates. The robust model demonstrates a remarkably similar behavior pattern to the deterministic model across the spectrum of increasing costs, suggesting its effectiveness in optimizing relay placement even as financial constraints intensify. As we can see in the trend of Z_{AC}, if we consider the robust solution in a deterministic situation, the average increase in objective value is 247.89 with a standard deviation of 0.61. In contrast, if we consider the trend of Z_{WC}, which represents the deterministic solution in the worst case, the increase in objective value is 3652.10 with a standard deviation of 0.89. This comparison highlights the robust model's ability to provide near-optimal solutions while accounting for data uncertainties, a crucial advantage in real-world applications where perfect information is rarely available.

Further insights into the energy efficiency of our proposed two-stage robust approach are provided by Figure 20. Implementing a WBAN with our two-stage robust approach results in a modest average increase of 0.058 in energy consumption compared to the deterministic method, with a standard deviation of 0.006. This slight increase is justified by the model's ability to account for worst-case scenarios, as evidenced by the plateau observed in the R_{AC} curve. Conversely, developing a WBAN without considering data uncertainty could lead to worst-case scenarios resulting in a significant loss of energy resources—an average of 0.8026 in energy consumption, with a standard deviation of 0.082, as depicted by the R_{WC} curve. This stark contrast shows that the energy consumption increase in our robust approach is substantially lower than in the worst-case scenario, highlighting its efficiency and practicality.

The divergence in performance between the robust and worst-case models highlights the critical importance of selecting an appropriate modeling approach in relay placement optimization. While the robust model's resilience to cost increases and its ability to maintain near-optimal solutions make it a reliable choice for long-term planning and variable economic conditions, the worst-case model's sensitivity to cost parameters suggests its utility may be limited to specific, highly conservative planning scenarios.

These findings emphasize the need for careful model selection in infrastructure planning, particularly when dealing with increasing costs and uncertain economic environments. The robust model's ability to maintain optimality closely aligned with the deterministic approach, even under increasing financial pressure, while also accounting for data uncertainties, makes it a better choice for practical applications in relay network design and optimization.

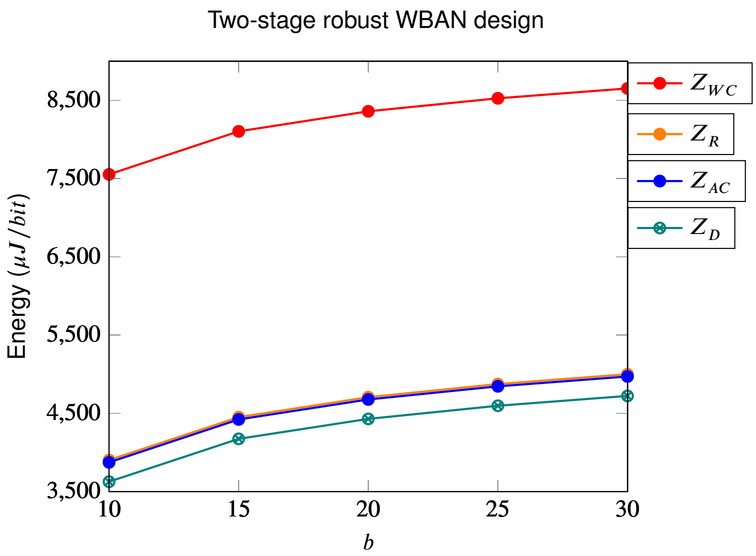

Figure 19: Comparison of Z_D, Z_R, Z_{AC}, and Z_{WC} as a function of relay installation costs (b parameter in eq. (33)).

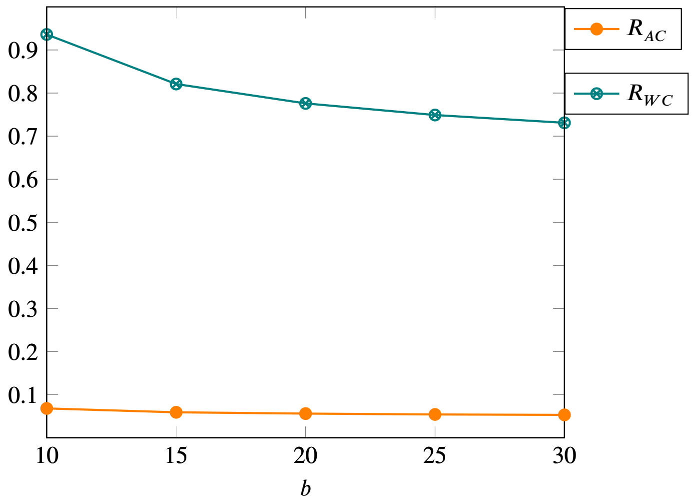

Figure 20: Comparison of R_{AC} and R_{WC} as a function of relay installation costs (b parameter in eq. (33)).

Impact of Increasing Nominal Traffic Demand in the Intersection Uncertainty Model

In this section, we explore the effects of increasing nominal traffic demand in the intersection uncertainty model by augmenting the nominal data rate ($\overline{d^b}$) by 25%, 50%, 75%, and 100%. Specifically, we modify such parameter as follows:

$$\text{New Nominal Data Rate} = \alpha \cdot \overline{d^b} \quad \text{for} \quad \alpha \in \{1, 1.25, 1.5, 1.75, 2.0\}. \tag{34}$$

For this analysis, we set the parameters in our logarithmic cost function (33) to $a = 200$ and $b = 30$. Additionally, for all scenarios, we fix the uncertainty level to the maximum value considered in this work, that is, $\rho_b = 0.9$.

Figure 21 illustrates a comparative analysis of the robust, deterministic, and worst-case models as the nominal data rate increases. As we can see in the trend of Z_{AC}, if we consider the robust solution in a deterministic situation, the average increase in objective value is 770.88 with a standard deviation of 504.84. In contrast, if we consider the trend of Z_{WC}, which represents the deterministic solution in the worst case, the increase in objective value is 3406.79 with a standard deviation of 534.89.

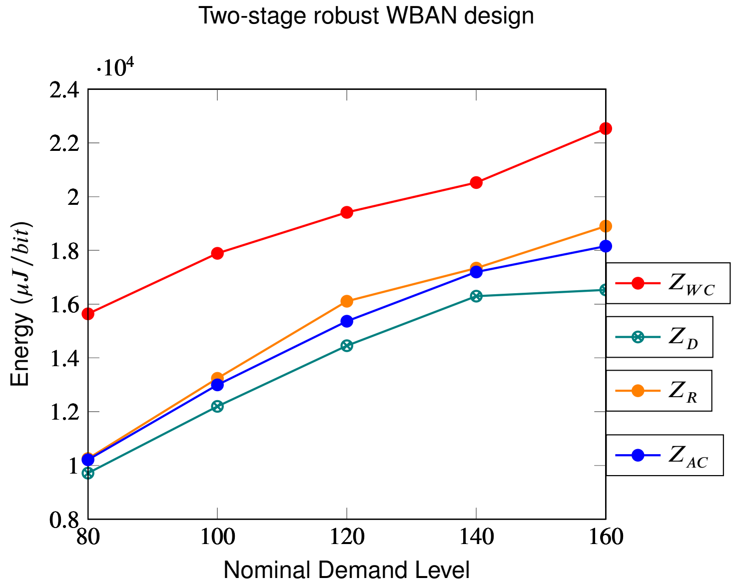

Figure 21: Comparison of Z_D, Z_R, Z_{AC}, and Z_{WC} as a function of nominal demand levels ranging from 80 to 160.

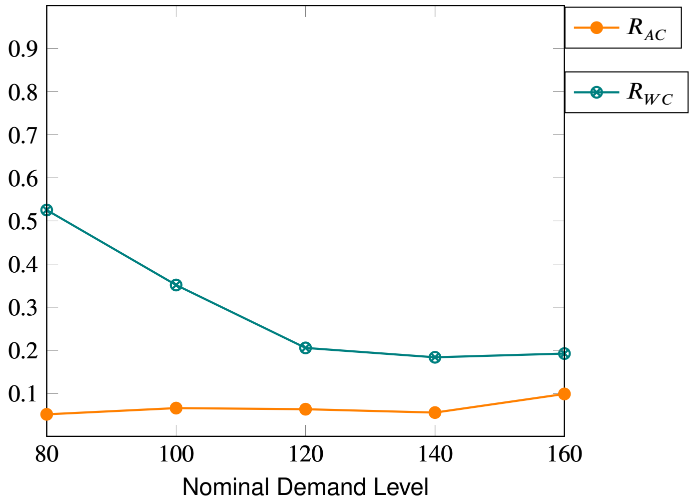

Figure 22: Comparison of R_{AC} and R_{WC} as a function of nominal demand levels ranging from 80 to 160

Further insights into the energy efficiency of our proposed two-stage robust approach are provided by Figure 22. Implementing a WBAN with this method results in a modest average increase of 0.0667 in energy consumption compared to the deterministic method, with a standard deviation of 0.0187 (R_{AC} curve). On the other hand, worst-case scenarios lead to a significant loss of energy resources—averaging a detrimental increase of 0.2915 with a standard deviation of 0.1477 (R_{WC} curve).

These findings highlight the effectiveness of the robust model in maintaining optimality and energy efficiency even when nominal traffic demand is increased significantly. While all models—deterministic, two-stage robust, and worst-case—exhibit similar behavior when nominal traffic demand rises, the key distinction of our two-stage robust model lies in its superior capability to manage the expanded uncertainty region. The results suggest that our two-stage robust approach can effectively manage uncertainty while minimizing both cost and energy consumption in practical WBAN implementations.

	N_R					
	$\rho_b = 0.3$		$\rho_b = 0.6$		$\rho_b = 0.9$	
Model	Polyhedral	Intersection	Polyhedral	Intersection	Polyhedral	Intersection
Deterministic	7	7	7	7	7	7
Robust	7	8	7	10	7	7
Worst-case	7	7	7	7	7	7

(a) Number of relays installed by the deterministic model, the two-stage robust model and the worst-case scenario under different levels of uncertainty $\rho_d = \{0.3, 0.6, 0.9\}$.

ρ_d	Polyhedral uncertainty set (%)				Intersection uncertainty set (%)			
	v^1	v^2	v^3	v^4	v^1	v^2	v^3	v^4
0.3	14.3	57	14.3	14.4	12.5	75	0	12.5
0.6	28.6	42.9	0	28.5	30	60	10	0
0.9	28.6	28.6	14.2	28.6	14.3	42.9	14.2	28.6

(b) Percentage of relays installed with type v^1, v^2, v^3 and v^4 by the two-stage robust WBAN design model.

Table 4
Number (a) and percentage (b) of installed relays with different capacity values.

Discussion on the Two-Stage Robust model: Relay number and installed capacity comparison

To highlight and summarize the dependency of the robust model's performance on the considered uncertainty sets and the impact of these latter on the behavior of the model, in terms of selecting appropriate capacities for relays before the realization of the actual data values, we finally focus on comparing the number and types of relays installed in the network and their variation with changes in uncertainty levels for the robust model considering both polyhedral and intersection uncertainty sets. The results are summarized in Table 4 for different uncertainty levels, $\rho_d = \{0.3, 0.6, 0.9\}$. It can be observed that the worst-case model, which aims to minimize relay installation costs, installs the minimum number of relays. As a results, the deterministic model and the worst-case scenario end up with the same number of installed relays in this situation. However, it is important to note that the capacities of the relays installed for the worst-case scenario vary based on the level of uncertainty, with a preference for installing higher-capacity relays. The Robust model under the polyhedral uncertainty set, independently from the uncertainty level and similarly to the deterministic model and the worst-case scenario, installs only 7 relays. However, the relay capacity types change with the uncertainty level. Under the polyhedral uncertainty set, the robust model has acceptable control over the number of installed relays and the appropriate capacity selection for them. In fact, more than 70% of the relays are installed with the lowest capacity (and hence lowest cost) while $\rho_d = 0.3$ and $\rho_d = 0.6$. When the uncertainty level reaches 0.9, only 10% of the relays have been replaced with the maximum capacity ones. Compared to the two-stage Robust model under polyhedral uncertainty set, the number of installed relays changes with respect to the uncertainty level in the Intersection set: under such set our model installed 8, 10, and 7 relays with $\rho_d = 0.3$, $\rho_d = 0.6$, and $\rho_d = 0.9$, respectively. Based on the data in the Table, the Robust model under the intersection uncertainty set installs nearly 90% of the relays with the lowest capacity (types v^1 and v^2) for $\rho_d = 0.3$, and $\rho_d = 0.6$, respectively. Finally, when the worst uncertainty occurs ($\rho_d = 0.9$), the intersection model behaves similarly to the polyhedral one. Overall, we can conclude that applying our proposed two-stage robust approach to WBANs, under both Polyhedral and Intersection uncertainty sets, effectively designs a flexible network by accurately selecting the relay capacities. This results in a lower investment cost and reduced energy consumption, even in worst-case scenarios.

8. Conclusions and Futures Research Directions

This paper proposes a two-stage Robust programming model for capacity planning in Wireless Body Area Networks (WBANs). The model focuses on optimizing energy consumption and relay placement costs while addressing uncertainties in data rates. By framing the problem as a two-stage stochastic programming with recourse, the model determines relay capacities in the first stage and decides on relay placement and data routing in the second stage to meet actual data requirements under uncertain conditions. This approach aligns with the broader context of network design problems with uncertain parameters, specifically addressing the critical data transmission needs of WBANs. The two-stage robust programming model offers a suitable framework for managing uncertainties in data transmission rates through relay nodes, enhancing the efficiency and reliability of WBAN design.

In the context of stochastic data generation, we tackle relay capacity selection and network lifetime as fundamental issues concerning WBAN quality of services. Initially, we formulate the model as a mixed-integer linear programming problem aimed at optimizing relay node placement and identifying efficient routing strategies through multi-hop routing techniques. However, numerical findings indicate that this formulation is overly conservative, leading to limitations in extending network lifetime under worst-case scenarios of data-driven uncertainties. Additionally, the selection of relay capacities is not cost-effective, often requiring the installation of high-capacity and costly relays to handle substantial traffic volumes in each transmission.

To address these challenges and effectively manage fluctuations between planned and actual data, we introduce the concept of Two-stage robust optimization in our proposed model. Our key assumption involves integrating uncertain data, a critical aspect of WBANs, into two predefined uncertainty sets. We present a robust formulation with the primary assumption focusing on uncertain demand within specified closed, convex, and bounded uncertainty sets. Given this uncertainty, we naturally segregate decision variables y (first stage) from variables x, z, and f (second stage).

The study demonstrates that the two-stage robust model optimizes WBANs efficiently. Under the polyhedral uncertainty set, the model shows only a 6.4% increase in energy consumption for nominal parameters, maintaining more than 71% of relays with the lowest capacity at uncertainty levels $\rho_d = 0.3$ and $\rho_d = 0.6$. Under the intersection uncertainty set, 87.5% and 90% of relays have the lowest capacity for $\rho_d = 0.3$ and $\rho_d = 0.6$, respectively. Even at the highest uncertainty ($\rho_d = 0.9$), the model ensures robust network performance with minimal adjustments, keeping investment costs low and energy consumption efficient.

Future Research Directions

This study presents a two-stage robust optimization framework for Wireless Body Area Networks (WBANs), focusing on demand uncertainty, energy efficiency, and network reliability. While these contributions provide a strong foundation, future research could explore additional dimensions to enhance the performance, resilience, and adaptability of WBANs.

A critical area for further investigation is the concept of resilience, defined in seminal works such as "Toward a Resilient Manufacturing System" [Zhang and van Luttervelt, 2011] as a network's intrinsic ability to sustain required operations under both expected and unexpected disruptions. Building on concepts from resilience engineering, future work could explore fault tolerance by designing mechanisms to ensure uninterrupted operation despite node failures or connectivity disruptions. Self-healing networks, capable of dynamic reconfiguration and restoration of functionality following failures or environmental disturbances, represent another promising direction. Additionally, adaptive performance mechanisms could be developed to enable WBANs to respond dynamically to environmental changes, interference, or unexpected traffic demands. These aspects align with resilience paradigms in complex systems and could be quantitatively analyzed using metrics adapted from resilient manufacturing systems.

Resilient communication within WBANs is vital, especially under conditions of interference, mobility, or partial network failures. Future studies could focus on developing adaptive and fault-tolerant routing protocols that ensure robust data transmission under uncertain or deteriorating conditions. Introducing hierarchical or cooperative strategies for routing could further enhance overall network resilience while optimizing energy consumption.

The current study addresses uncertainty in demand. However, WBANs are subject to diverse uncertainty factors, including channel variations due to signal degradation caused by body movement or external interference, energy constraints such as those arising in energy-harvesting scenarios, and mobility patterns reflecting dynamic changes in sensor placement or user activities. Integrating these dimensions into robust optimization models would better capture the complexity of real-world WBAN deployments.

Energy efficiency is a cornerstone of WBAN design. Future research could focus on developing energy-aware frameworks that incorporate resilience by dynamically reallocating resources or optimizing power consumption during failures. Advanced energy-harvesting techniques and adaptive duty-cycling mechanisms could be integrated to ensure prolonged network operation under uncertain conditions.

Balancing multiple objectives, such as cost, energy efficiency, and resilience, remains a challenging but essential task. Future efforts could develop multi-objective optimization models that explicitly incorporate resilience metrics alongside traditional performance criteria. These models could be used to evaluate trade-offs, ensuring WBANs are both cost-effective and robust under varying operational scenarios.

The adoption of stochastic and dynamic uncertainty sets in robust optimization could further enhance the adaptability of WBANs. Future research could investigate techniques for real-time adjustment of uncertainty sets, enabling WBANs to adapt to evolving environmental and operational conditions. Hybrid models that combine robust and stochastic optimization could be explored to handle both predictable and unpredictable uncertainties effectively.

By addressing these research directions, WBANs can evolve into systems capable of maintaining high performance, efficiency, and resilience, even in the face of complex and dynamic real-world challenges.

Acknowledgment

This research was funded by the University of Montpellier's MAK'IT (Montpellier Advanced Knowledge Institute on Transitions) visiting scientist program, by project SERICS (PE00000014) under the NRRP MUR program funded by the EU - NGEU. Also, it was partly supported by PRIN Project NEWTON (2022ZA8T22).

CRediT authorship contribution statement

Mohammad Ali Raayatpanah: Conceptualization, Methodology, Software, Writing – Original Draft, Writing – Review and Editing. **Atefeh Abdolah Abyaneh:** Numerical Analysis, Results, Writing – Original Draft, Writing – Review and Editing. **Jocelyne Elias:** Supervision, Writing – Review and Editing, Quality Improvement. **Fabio Martignon:** Supervision, Writing – Review and Editing, Quality Improvement.

References

Shashank Kumar, Arjit Kaur Arora, Parth Gupta, and Baljit Singh Saini. *A Review of Applications, Security and Challenges of Internet of Medical Things*, pages 1–23. Springer International Publishing, Cham, 2021. ISBN 978-3-030-55833-8.

Sahshanu Razdan and Sachin Sharma. Internet of Medical Things (IoMT): overview, emerging technologies, and case studies. *IETE Technical Review*, 39(4):775–788, 2022.

Sonam Lata, Shabana Mehfuz, and Shabana Urooj. Secure and Reliable WSN for Internet of Things: Challenges and Enabling Technologies. *IEEE Access*, 9:161103–161128, 2021.

G. Elhayatmy, Nilanjan Dey, and Amira S. Ashour. Internet of Things Based Wireless Body Area Network in Healthcare. In Nilanjan Dey, Aboul Ella Hassanien, Chintan Bhatt, Amira S. Ashour, and Suresh Chandra Satapathy, editors, *Internet of Things and Big Data Analytics Toward Next-Generation Intelligence*, pages 3–20. Springer International Publishing, Cham, 2018. ISBN 978-3-319-60435-0.

Rajeev Sharma and Sandeep Singh Kang. WBAN for healthcare applications: A survey of current challenges and research opportunities. *Journal of Critical Reviews*, 7(17):2444–2453, 2020.

M Alper Akkaş, Radosveta Sokullu, and H Ertürk Cetin. Healthcare and patient monitoring using IoT. *Internet of Things*, 11:100173, 2020. ISSN 2542-6605. doi: https://doi.org/10.1016/j.iot.2020.100173. URL https://www.sciencedirect.com/science/article/pii/S2542660520300147.

Jianhong Zhang and Chenghe Dong. Secure and Lightweight Data Aggregation Scheme for Anonymous Multi-Receivers in WBAN. *IEEE Transactions on Network Science and Engineering*, 10:81–91, 2023. doi: 10.1109/TNSE.2022.3205044.

Onorato d'Angelis, Lazzaro Di Biase, Luca Vollero, and Mario Merone. IoT architecture for continuous long term monitoring: Parkinson's Disease case study. *Internet of Things*, 20:100614, 2022. ISSN 2542-6605. doi: https://doi.org/10.1016/j.iot.2022.100614. URL https://www.sciencedirect.com/science/article/pii/S2542660522000968.

Antonio Iyda Paganelli, Pedro Elkind Velmovitsky, Pedro Miranda, Adriano Branco, Paulo Alencar, Donald Cowan, Markus Endler, and Plinio Pelegrini Morita. A conceptual IoT-based early-warning architecture for remote monitoring of COVID-19 patients in wards and at home. *Internet of Things*, 18:100399, 2022. ISSN 2542-6605. doi: https://doi.org/10.1016/j.iot.2021.100399. URL https://www.sciencedirect.com/science/article/pii/S2542660521000433.

K. Narendra Swaroop, Kavitha Chandu, Ramesh Gorrepotu, and Subimal Deb. A health monitoring system for vital signs using IoT. *Internet of Things*, 5:116–129, 2019. ISSN 2542-6605. doi: https://doi.org/10.1016/j.iot.2019.01.004. URL https://www.sciencedirect.com/science/article/pii/S2542660518300349.

Farman Ullah, M Zahid Khan, Gulzar Mehmood, Muhammad Shuaib Qureshi, and Muhammad Fayaz. Energy Efficiency and Reliability Considerations in Wireless Body Area Networks: A Survey. *Computational and Mathematical Methods in Medicine*, 2022:1–15, 2022. doi: 10.1155/2022/1090131.

Fasee Ullah, Z. Ullah, Sheeraz Ahmad, Ihtesham Ul Islam, S. Rehman, and Javed Iqbal. Traffic priority based delay-aware and energy efficient path allocation routing protocol for wireless body area network. *Journal of Ambient Intelligence and Humanized Computing*, pages 1–20, 2019. doi: 10.1007/s12652-019-01343-w.

Yang Zhou, Zhengguo Sheng, Chinmaya Mahapatra, Victor CM Leung, and Peyman Servati. Topology design and cross-layer optimization for wireless body sensor networks. *Ad Hoc Networks*, 59:48–62, 2017. doi: 10.1016/j.adhoc.2017.01.005.

N. Kaur and Sukhwinder Singh. Optimized cost effective and energy efficient routing protocol for wireless body area networks. *Ad Hoc Networks*, 61:65–84, 2017. doi: 10.1016/j.adhoc.2017.03.008.

Sye Loong Keoh, Kevin Twidle, Nathaniel Pryce, Alberto E Schaeffer-Filho, Emil Lupu, Naranker Dulay, Morris Sloman, Steven Heeps, Stephen Strowes, Joe Sventek, et al. Policy-based management for body-sensor networks. In *4th International Workshop on Wearable and Implantable Body Sensor Networks (BSN 2007) March 26–28, 2007 RWTH Aachen University, Germany*, pages 92–98. Springer, 2007.

Urbashi Mitra, B Adar Emken, Sangwon Lee, Ming Li, Viktor Rozgic, Gautam Thatte, Harshvardhan Vathsangam, Daphney-Stavroula Zois, Murali Annavaram, Shrikanth Narayanan, et al. KNOWME: a case study in wireless body area sensor network design. *IEEE Communications Magazine*, 50(5):116–125, 2012. doi: 10.1109/MCOM.2012.6194391.

Min Chen, S. González-Valenzuela, A. Vasilakos, Huasong Cao, and Victor C. M. Leung. Body Area Networks: A Survey. *Mobile Networks and Applications*, 16:171–193, 2010. doi: 10.1007/S11036-010-0260-8.

Fabio D'Andreagiovanni and Antonella Nardin. Towards the fast and robust optimal design of wireless body area networks. *Applied Soft Computing*, 37:971–982, 2015. doi: 10.1016/j.asoc.2015.04.037.

Eduardo Feo Flushing and Gianni A Di Caro. Relay node placement for performance enhancement with uncertain demand: A robust optimization approach. In *2013 11th International Symposium and Workshops on Modeling and Optimization in Mobile, Ad Hoc and Wireless Networks (WiOpt)*, pages 556–563. IEEE, 2013.

R. A. Khan, Qin Xin, and Nabiha Roshan. RK-Energy Efficient Routing Protocol for Wireless Body Area Sensor Networks. *Wireless Personal Communications*, 116:709–721, 2020. doi: 10.1007/s11277-020-07734-z.

M Abdul Jawad and Farida Khurshid. A review of approaches to energy aware multi-hop routing for lifetime enhancement in wireless sensor networks. In *Proceedings of the International e-Conference on Intelligent Systems and Signal Processing*, pages 739–757. Springer, 2022.

Avani Vyas, Sujata Pal, and Barun Kumar Saha. Relay-based communications in wbans: A comprehensive survey. *ACM Computing Surveys (CSUR)*, 54(1):1–34, 2021.

Mohammad Ali Raayatpanah, Atefeh Abdolah Abyaneh, Jocelyne Elias, and Angelo Trotta. Optimal reliable design of energy-efficient wireless body area networks. *Internet of Things*, 22:100727, 2023. doi: https://doi.org/10.1016/j.iot.2023.100727. URL https://www.sciencedirect.com/science/article/abs/pii/S2542660523000501.

Amit Samanta and Sudip Misra. Energy-efficient and distributed network management cost minimization in opportunistic wireless body area networks. *IEEE Transactions on Mobile Computing*, 17(2):376–389, 2018. doi: 10.1109/TMC.2017.2708713.

Suvrajeet Sen, Robert D Doverspike, and Steve Cosares. Network planning with random demand. *Telecommunication systems*, 3(1):11–30, 1994. doi: https://doi.org/10.1007/BF02110042. URL https://link.springer.com/article/10.1007/BF02110042.

Abdel Lisser, Adamou Ouorou, Jean-Philippe Vial, Jacek Gondzio, et al. *Capacity planning under uncertain demand in telecommunication networks*. HEC Genève, 1999.

Morten Riis and Kim Allan Andersen. Capacitated network design with uncertain demand. *INFORMS Journal on Computing*, 14(3):247–260, 2002. doi: https://doi.org/10.1287/ijoc.14.3.247.111. URL https://pubsonline.informs.org/doi/abs/10.1287/ijoc.14.3.247.111.

Huasong Cao, Victor C. M. Leung, C. C. Chow, and Henry C. B. Chan. Enabling technologies for wireless body area networks: A survey and outlook. *IEEE Communications Magazine*, 47, 2009. doi: 10.1109/MCOM.2009.5350373.

B. Liu, Zhisheng Yan, and Chang Wen Chen. MAC protocol in wireless body area networks for E-health: challenges and a context-aware design. *IEEE Wireless Communications*, 20:64–72, 2013. doi: 10.1109/MWC.2013.6590052.

Steffen Peter, Bhanu Pratap Reddy, F. Momtaz, and T. Givargis. Design of Secure ECG-Based Biometric Authentication in Body Area Sensor Networks. *Sensors (Basel, Switzerland)*, 16, 2016. doi: 10.3390/s16040570.

R. A. Khan and A. Pathan. The state-of-the-art wireless body area sensor networks: A survey. *International Journal of Distributed Sensor Networks*, 14, 2018. doi: 10.1177/1550147718768994.

Hisham Alshaheen and Haifa Takruri-Rizk. Improving the energy efficiency for biosensor nodes in the WBSN bottleneck zone based on a random linear network coding. *2017 11th International Symposium on Medical Information and Communication Technology (ISMICT)*, pages 59–63, 2017. doi: 10.1109/ISMICT.2017.7891767. URL https://api.semanticscholar.org/CorpusID:14362309.

M. Kanthi and Ravilla Dilli. Wearable Biosensor: How to Improve the Efficacy in Data Transmission in Respiratory Monitoring System? *International Journal of Electronics and Telecommunications*, 69(1):25–32, 2023.

Jiahui Hu, Qing Qian, An Fang, Sizhu Wu, and Yi Xie. Optimal data transmission strategy for healthcare-based wireless sensor networks: A stochastic differential game approach. *Wireless Personal Communications*, 89:1295–1313, 2016. doi: DOI: 10.24425/ijet.2023.144327.

Adhikary S. Chattopadhyay S. Choudhury S. Ghosh, B. Achieving Energy Efficiency and Impact of SAR in a WBAN Through Optimal Placement of the Relay Node. *Wireless Personal Communications*, 130:1861–1884, 2023.

Zhong Liang D. Memon K.A. et al Panhwar, M.A. Energy-efficient routing optimization algorithm in WBANs for patient monitoring. *Journal of Ambient Intelligence and Humanized Computing*, 12:8069–8081, 2021.

Samal T. Kabat M.R. et al Patra, S.C. Optimizing relay node placement and routing in WBANs using free search krill herd and harmony search algorithm. *Multimedia Tools and Applications*, 2024.

Bin Han, Wenjun Zhang, Xiwen Lu, and Yingzi Lin. On-line supply chain scheduling for single-machine and parallel-machine configurations with a single customer: Minimizing the makespan and delivery cost. *European Journal of Operational Research*, 244(3):704–714, 2015. ISSN 0377-2217. doi: https://doi.org/10.1016/j.ejor.2015.02.008. URL https://www.sciencedirect.com/science/article/pii/S0377221715001058.

W.J. Zhang and C.A. van Luttervelt. Toward a resilient manufacturing system. *CIRP Annals*, 60(1):469–472, 2011. ISSN 0007-8506. doi: https://doi.org/10.1016/j.cirp.2011.03.041. URL https://www.sciencedirect.com/science/article/pii/S0007850611000424.

JW Wang, HF Wang, YM Zhou, Y Wang, and Wen-Jun Zhang. On an integrated approach to resilient transportation systems in emergency situations. *Natural computing*, 18:815–823, 2019.

Tan Zhang, Wenjun Zhang, and Madan M Gupta. An underactuated self-reconfigurable robot and the reconfiguration evolution. *Mechanism and Machine Theory*, 124:248–258, 2018.

Amit Samanta, Thanh Phung Truong, Nhu-Ngoc Dao, and Sungrae Cho. Loss-aware adaptive load balancing scheme for iot-enabled wbans with qos-factor. In Nhu-Ngoc Dao, Quang-Dung Pham, Sungrae Cho, and Ngoc Thanh Nguyen, editors, *Intelligence of Things: Technologies and Applications*, pages 262–274, Cham, 2024. Springer Nature Switzerland. ISBN 978-3-031-75593-4.

Aharon Ben-Tal, Laurent El Ghaoui, and Arkadi Nemirovski. *Robust optimization*, volume 28. Princeton university press, 2009a.

John R Birge and Francois Louveaux. *Introduction to stochastic programming*. Springer Science & Business Media, 2011. doi: https://doi.org/10.1007/978-1-4614-0237-4.

Dimitris Bertsimas and Melvyn Sim. Robust discrete optimization and network flows. *Mathematical Programming*, 98:49–71, 09 2003. doi: 10.1007/s10107-003-0396-4.

A Ben-Tal, Laurent El Ghaoui, and Arkadii Semenovich Nemirovskii. *Robust optimization*. Princeton University Press, 2009b.

Aharon Ben-Tal and Arkadi Nemirovski. Robust convex optimization. *Mathematics of operations research*, 23(4):769–805, 1998. doi: https://doi.org/10.1287/moor.23.4.769. URL `https://pubsonline.informs.org/doi/10.1287/moor.23.4.769`.

Laurent El Ghaoui, Francois Oustry, and Hervé Lebret. Robust Solutions to Uncertain Semidefinite Programs. *SIAM Journal on Optimization*, 9 (1):33–52, 1998. doi: 10.1137/S1052623496305717. URL `https://doi.org/10.1137/S1052623496305717`.

Dimitris Bertsimas and Melvyn Sim. The price of robustness. *Operations research*, 52(1):35–53, 2004. doi: https://doi.org/10.1287/opre.1030.0065. URL `https://pubsonline.informs.org/doi/abs/10.1287/opre.1030.0065`.

Amit Samanta, Flavio Esposito, and Tri Gia Nguyen. Fault-tolerant mechanism for edge-based iot networks with demand uncertainty. *IEEE Internet of Things Journal*, 8(23):16963–16971, 2021.

Tazar Hussain, Chris Nugent, Adrian Moore, and Jun Liu. An analysis of the impact of uncertainty on the internet of things: A smart home case study. In *2019 IEEE SmartWorld, Ubiquitous Intelligence & Computing, Advanced & Trusted Computing, Scalable Computing & Communications, Cloud & Big Data Computing, Internet of People and Smart City Innovation (SmartWorld/SCALCOM/UIC/ATC/CBDCom/IOP/SCI)*, pages 1916–1921. IEEE, 2019.

Ghalya Alwhishi, Jamal Bentahar, and Nagat Drawel. Reasoning about uncertainty over iot systems. In *2022 International Wireless Communications and Mobile Computing (IWCMC)*, pages 306–311. IEEE, 2022.

Cai Xu, Wei Zhao, Jinglong Zhao, Ziyu Guan, Xiangyu Song, and Jianxin Li. Uncertainty-aware multiview deep learning for internet of things applications. *IEEE Transactions on Industrial Informatics*, 19(2):1456–1466, 2022.

A. Ben-Tal, A. Goryashko, E. Guslitzer, and A. Nemirovski. Adjustable robust solutions of uncertain linear programs. *Mathematical Programming*, 99:351–376, 2004. doi: 10.1007/s10107-003-0454-y.

Alper Atamtürk and Muhong Zhang. Two-Stage Robust Network Flow and Design Under Demand Uncertainty. *Operations Research*, 55:662–673, 08 2007. doi: 10.1287/opre.1070.0428.

Osama Amjad, Ebrahim Bedeer, Najah Abu Ali, and Salama Ikki. Robust energy efficiency optimization algorithm for health monitoring system with wireless body area networks. *IEEE Communications Letters*, 24(5):1142–1145, 2020. doi: https://doi.org/10.1109/LCOMM.2020.2971493. URL `https://ieeexplore.ieee.org/abstract/document/8981867`.

Omar Ahmed, Fuji Ren, Ammar Hawbani, and Yaser Al-Sharabi. Energy optimized congestion control-based temperature aware routing algorithm for software defined wireless body area networks. *IEEE Access*, 8:41085–41099, 2020. doi: 10.1109/ACCESS.2020.2976819.

Jocelyne Elias. Optimal design of energy-efficient and cost-effective wireless body area networks. *Ad Hoc Networks*, 13:560–574, 2014.

Elisabeth Reusens, Wout Joseph, Benoît Latré, Bart Braem, Günter Vermeeren, Emmeric Tanghe, Luc Martens, Ingrid Moerman, and Chris Blondia. Characterization of on-body communication channel and energy efficient topology design for wireless body area networks. *IEEE Transactions on Information Technology in Biomedicine*, 13(6):933–945, 2009.

Jocelyne Elias, Abdallah Jarray, Javier Salazar, Ahmed Karmouch, and Ahmed Mehaoua. A reliable design of wireless body area networks. In *2013 IEEE Global Communications Conference (GLOBECOM)*, pages 2742–2748. IEEE, 2013.

A. Ben-Tal and A. Nemirovski. Robust solutions of uncertain linear programs. *Operations Research Letters*, 25:1–13, 1999. doi: 10.1016/S0167-6377(99)00016-4.

Sanjula Kammammettu and Zukui Li. Two-stage robust optimization of water treatment network design and operations under uncertainty. *Industrial Engineering Chemistry Research*, 59:1218–1233, 2020. doi: 10.1021/acs.iecr.9b05365.

A. Jabbarzadeh, M. Haughton, and Fahime Pourmehdi. A robust optimization model for efficient and green supply chain planning with postponement strategy. *International Journal of Production Economics*, 2019. doi: 10.1016/J.IJPE.2018.06.013.

Hongxu Huang, Liang Rui, Chaoxian Lv, Lu Mengtian, Dunwei Gong, and Shulin Yin. Two-stage robust stochastic scheduling for energy recovery in coal mine integrated energy system. *Applied Energy*, 290:116759, 2021. doi: 10.1016/J.APENERGY.2021.116759.

Aharon Ben-Tal, Stephen Boyd, and Arkadi Nemirovski. Extending scope of robust optimization: Comprehensive robust counterparts of uncertain problems. *Mathematical Programming*, 107:63–89, 2006. doi: 10.1007/s10107-005-0679-z.

Dimitris Bertsimas and David B Brown. Constructing uncertainty sets for robust linear optimization. *Operations research*, 57(6):1483–1495, 2009. doi: 10.1287/opre.1080.0646.

Amir Jalilvand-Nejad, R. Shafaei, and H. Shahriari. Robust optimization under correlated polyhedral uncertainty set. *Comput. Ind. Eng.*, 92:82–94, 2016. doi: 10.1016/j.cie.2015.12.006.

Dimitris Bertsimas and John N Tsitsiklis. *Introduction to linear optimization*. Athena Scientific, 1997.

M S Bazaraa, John J Jarvis, and Hanif D Sherali. *Linear programming and network flows*. John Wiley & Sons, 2010.

Walid Ben-Ameur and Hervé Kerivin. New economical virtual private networks. *Association for Computing Machinery. Communications of the ACM*, 46(6):69–69, 2003.

Walid Ben-Ameur, Adam Ouorou, and Mateusz Zotkiewicz. Robust routing in communication networks. In *Progress in combinatorial optimization*, pages 353 – 390. Iste; Wiley, 2011. URL https://hal.science/hal-01279133.

Lisha Zhong, Shuling He, Jinzhao Lin, Jia Wu, Xi Li, Yu Pang, and Zhangyong Li. Technological Requirements and Challenges in Wireless Body Area Networks for Health Monitoring: A Comprehensive Survey. *Sensors (Basel, Switzerland)*, 22, 2022. doi: 10.3390/s22093539.

Benoît Latré, Bart Braem, Ingrid Moerman, Chris Blondia, and Piet Demeester. A survey on wireless body area networks. *Wireless networks*, 17:1–18, 2011. doi: https://doi.org/10.1287/opre.1030.0065. URL https://link.springer.com/article/10.1007/s11276-010-0252-4.

Md Taslim Arefin, Mohammad Hanif Ali, and AKM Fazlul Haque. Wireless body area network: An overview and various applications. *Journal of Computer and Communications*, 5(7):53–64, 2017.

Rasmita Kumari Mohanty, Satya Prakash Sahoo, and Manas Ranjan Kabat. Sustainable remote patient monitoring in wireless body area network with multi-hop routing and scheduling: a four-fold objective based optimization approach. *Wireless Networks*, pages 1–15, 2023. doi: 10.1007/s11276-023-03276-x. URL https://link.springer.com/article/10.1007/s11276-023-03276-x.

Zeinab Shahbazi and Yung-Cheol Byun. Towards a secure thermal-energy aware routing protocol in wireless body area network based on blockchain technology. *Sensors*, 20(12):1–26, 2020.

Tushar Kanta Samal, Sushree Chinmayee Patra, and Manas Ranjan Kabat. An adaptive cuckoo search based algorithm for placement of relay nodes in wireless body area networks. *Journal of King Saud University-Computer and Information Sciences*, 2019.

Tin-Yu Wu and Cheng-Han Lin. Low-SAR path discovery by particle swarm optimization algorithm in wireless body area networks. *IEEE Sensors Journal*, 15(2):928–936, 2014.

Ghufran Ahmed, Saif Ul Islam, Maham Shahid, Adnan Akhunzada, Sohail Jabbar, Muhammad Khurram Khan, Muhammad Riaz, and Kijun Han. Rigorous analysis and evaluation of specific absorption rate (SAR) for mobile multimedia healthcare. *IEEE Access*, 6:29602–29610, 2018. doi: 10.1109/ACCESS.2018.2839909. URL https://ieeexplore.ieee.org/abstract/document/8362927.

Ramanpreet Kaur, Bikram Pal Kaur, Ruchi Pasricha Singla, and Jaskirat Kaur. AMERP: Adam moment estimation optimized mobility supported energy efficient routing protocol for wireless body area networks. *Sustainable Computing: Informatics and Systems*, 31:100560, 2021.